Effect of Cellulose Fiber Addition on Autogenous Healing of Concrete and Their Use as a Bacteria-Carrier in Self-Healing Mortar

by

Harshbab Singh
Bachelor of Technology, Guru Nanak Dev Engineering College, 2012

A Thesis Submitted in Partial Fulfillment
of the Requirements for the Degree of

MASTER OF APPLIED SCIENCE
in the Department of Civil Engineering

Supervisory Committee

Effect of Cellulose Fiber Addition on Autogenous Healing of Concrete and Their Use as a Bacteria-Carrier in Self-Healing Mortar

by

Harshbab Singh

Bachelor of Technology, Guru Nanak Dev Engineering College, 2012

Supervisory Committee

Dr. Rishi Gupta, Department of Civil Engineering
Supervisor

Dr. Cheng Lin, Department of Civil Engineering
Departmental Member

Abstract

Crack formation under tensile forces is a major weakness of concrete. Cracks make concrete vulnerable to the extreme environment due to the ingress of water and harmful compounds from the surrounding environment. Conventional methods of crack repairing are expensive and time consuming. It is estimated that in Europe, cost related to repair works is half of the annual construction budget and the US has average annual maintenance cost for existing bridges through the year is estimated to $5.2 billion. To overcome this problem, a self-healing concrete is produced based on the application of mineral producing alkaliphilic *Bacillus Subtilis* (strain 168*)* bacteria. Metabolic activities of these bacteria on calcium-based nutrients results in precipitation of calcium carbonate, which helps to repair concrete cracks. In bacteria based self-healing concrete, the bacteria are protected in the dense cementitious matrix by encapsulating them in "bacteria-carriers". However, the presently available bacteria-carriers are not always suitable for concrete because of their complex manufacturing procedures or high cost. With the aim to develop a more suitable bacteria-carrier, in this study feasibility of cellulose fiber as a novel bacteria-carrier for self-healing mortar is investigated. Cellulose fibers compared to other bacteria-carriers can serve the dual purpose of arresting cracks and at the same time be a bacteria-carrier in large scale concrete construction. Two types of bacterial mortar by using cellulose fiber as a carrier was prepared. For one type, nutrients were added inside the mortar mix, while for the other, nutrients were added into the curing water. The two types of composites; control and cellulose fiber reinforced concrete (CeFRC) have also been investigated for autogenous healing of concrete. The crack healing efficiency of bacterial mortars was investigated using image analysis and ultrasonic pulse velocity (UPV) test and compared with unreinforced and control cellulose fiber mortars. Variation in compressive strength for all mixes compared to control mortar is also presented in this thesis. Research shows that self-sealing mortar using cellulose fiber as a bacteria-carrier result in maximum self-healing as compared to other mixes. This study also aims to evaluate the self-healing potential and water permeability of CeFRC. Compressive strength and flexural tests were also performed to evaluate the mechanical properties of the composites. Water

permeability test was used to evaluate the coefficient of permeability and the self-healing performance was investigated by using UPV and a patented self-healing test. The results indicate that the water permeability coefficient decreased by 42% (+15% or -21%) whereas the healing ratio increased at a higher rate for the initial days of healing when cellulose fibers were added in the concrete. CeFRC also results in a 7.8% increase in flexural strength.

Table of Contents

List of Tables

List of Figures

Acknowledgments

First, I would like to thank my Supervisor Dr. Rishi Gupta, Department of Civil Engineering, University of Victoria, for his guidance throughout my blessed journey. I am very thankful for his patience, continuous motivation and support in this research project. His guidance helped me in all the time of research and writing of this thesis.

Also, I would like to thank Dr. Francis Nano and Barb Currie from the Department of Biochemistry and Microbiology, University of Victoria, for their valuable help by providing the bacterial solutions for this research project.

I would like to express my gratitude to Dr. Armando Tura and Mr. Matthew Walker, Civil Engineering Technical Support, University of Victoria, for their assistance in laboratory activities.

I would like to thank all my colleagues of the Civil Engineering Research Group for their support in the obstacles of my journey. Special thanks go out to my colleague Peiman Azarsa for his valuable help in the material laboratory.

I am highly indebted to the Almighty, my family members and friends by whose blessings, endless love and support, help me to complete my study and encouraged me in all possible way.

Dedication

I would like to dedicate my thesis in loving memory of my grandfather

Chapter 1. Introduction

1.1 General

Cement/concrete is still one of the widely used materials in the construction industry. One downside, however, is that cement production alone contributes around 7% to global anthropogenic CO_2 emissions [1] and exerts negative impacts on the environment. Traditional concrete has another drawback, it tends to crack when subjected to tensile stresses. Cracking leads to an increase in permeability, decrease in durability and strength of the concrete structure. Due to the increase in the permeability, the water easily passes through the concrete matrix and comes in the contact with the reinforcement leading to corrosion initiation. Due to this, the strength of the concrete structure further decreases, necessitating repair of cracks [2]. Conventional repair methods use manual inspection followed by filling of cracks with cement or other synthetic fillers [1], which are very expensive and time consuming. It is estimated that in Europe, cost related to repair works is half of the annual construction budget [3]. The US has average annual maintenance cost for existing bridges through the year, which is estimated to $5.2 billion [4]. Additionally, indirect cost due to traffic jams and inconvenience is also associated with the concrete crack repair works. Therefore, to date the various self-healing repair methods including adhesive based, autogenous, mineral admixture based and bacteria based are developed to heal the cracks automatically without any external source [5, 6], and are helpful in decreasing the operational cost as compared to manual methods. Main mechanisms of autogenous self-healing are due to further hydration of unhydrated cement; recrystallization of portandite ($Ca(OH)_2$) leached from the bulk paste and formation of calcite [6], but autogenous self-healing can repair cracks to some extent only. Besides natural autogenous self-healing of concrete, bacteria based self-healing has become more popular recently because it has a better healing capacity and uses commonly available environment-friendly microbes.

Bacteria based self-healing works on the phenomenon of microbiologically induced calcite precipitation (MICP). MICP is a product of metabolic interactions of some microbial communities with organic or inorganic compounds present in the environment. A mineral producing alkaliphilic bacteria with calcium-based nutrients in cement mortar help

precipitation of calcium carbonate caused by metabolic activities of microbes. The precipitation of calcium carbonate helps to heal the cracks in cement mortar, resulting in an increase of the overall durability of the material. The MICP is feasible by two metabolic activities of bacteria, hydrolysis of urea [7] and working of bacteria on calcium-based nutrients [1]. In the former process, urea is used as a nutrient and results in the production of two ammonium ion for each carbonate ion during the formation of calcium carbonate, which results in the additional nitrogen loading and has a negative effect on the environment [1]. While in the latter case, the carbon dioxide is consumed and results in additional production of calcium carbonate. The advantage of this process when calcium lactate is used as a nutrient is that it does not have any impact on the setting time of concrete [8].

1.2 Need for Study

1.2.1 To study the autogenous self-healing of cellulose fiber reinforced concrete

The concept of using fibers to reinforce concrete has been used for hundreds of years. However, only a few studies have been performed to investigate the self-healing efficiency of fiber reinforced concrete [9, 10, 11]. Commonly used fibers in concrete are steel, glass, synthetic (polypropylene, polyethylene, nylon, and polyester) and naturals fibers (wood, fruit, cellulose), etc. Steel fibers improve the ductility, flexural strength and fracture toughness of concrete due to higher modulus of elasticity of steel; however, they are subjected to corrosion when comes in contact of water through cracks and their durability reduces. Although glass fiber enhances the tensile and impact strength of concrete, they became fragile with time due to the alkalinity of concrete [12]. Natural fibers used in concrete are eco-friendly, recyclable and widely available throughout the world at a much cheaper rate compared to other fiber types. Singh and Gupta [13] used the cellulose fiber as a carrier for bacteria in self-healing mortar to improve the self-healing efficiency of bacterial mortar. Cellulose fibers have the lower cost, 2706 USD/m^3 [14] as compared to steel (7110- 11850 USD/m^3) and glass fibers (3250 – 5000 USD/m^3) [15] . In this study, cellulose fibers are used as reinforcement and their impact on the autogenous self-healing of concrete is investigated.

1.2.2 To study the feasibility of cellulose fiber as a bacteria-carrier in self-healing mortar

A carrier is required to protect the bacteria from mechanical forces caused by mixing processes and hydration reaction in the cement matrix. Basically, methods to immobilize bacteria can be divided into two categories, encapsulated and absorbed depending upon the technique of immobilization, see Table 1.

Table 1: Bacteria-carriers used in different researches

Immobilization category	Bacteria-carrier	Encapsulation technique	Self-healing performance
Absorbed	Expanded Perlite (EP) [16]	Impregnated under vacuum, drying in an oven, coating with a geopolymer.	Completely healed crack width up to 0.79 mm after 28 days of healing
	Expanded Clay Pellets (EC) [17]	Impregnated under vacuum and drying in an oven	Completely healed crack width up to 0.46 mm after 100 days of healing
	Ceramsite [18]	Alkali erosion and sintering treatments, heat treatment at 750° C, soaking and drying in an oven	Maximum crack width healed 0.3 mm
Encapsulated	Epoxy [19]	Preparation of microcapsules by using in-situ polymerization procedure	Maximum crack healing 45% for crack size of 0.1 mm healed at 50º C.
	Hydrogel [20]	Mixing of spores with the polymer solution, addition of initiator, UV irradiation for 1 hour, freeze grinding and drying.	Maximum crack width healed 0.5 mm after 28 days.
	Melamine [21]	Preparation of microcapsules using a polycondensation reaction	Maximum crack width healed 0.97 mm.
	Polyurethane [22]	Mixing of spores with a two-component polyurethane to form PU foam	60% regain in the strength of cracked mortar specimen.

In the encapsulated method, bacteria and nutrients are immobilized in micro or macro capsules, spherical or cylindrical in shape. When crack hits these capsules, result in rupturing of the capsules and the bacteria and nutrients are released out, and precipitation takes place to heal the cracks [19]. However, the probability of crack hitting the capsule

is very low due to the limited number of capsules available in the crack region, especially for spherical capsule because they have less bond strength with the concrete matrix. On the other hand, cylindrical capsules have more bond strength with concrete, but they cause less release of nutrients due to the suction effect on the sealed end due to capillary forces [23]. Microcapsules are mainly manufactured using bulk emulsification polymerization techniques, but these methods have concerns related to capsule dimensions and bonding with the concrete matrix [24]. Also, these techniques required advanced equipment and complex procedures.

In the absorbed method, bacteria and nutrients are encapsulated in a porous material with high porosity by saturating the material with bacterial suspension. The highly porous material is helpful in providing enough space for bacteria growth, oxygen, and water, necessary for MICP.

To date, various carriers have been adopted like polyurethane [22], melamine [21], silica gel [22], expanded clay particles [8, 17], lightweight aggregates [25], graphite nano platelets [25], perlite [16], diatomaceous earth [26], and ceramsite [18] etc. The complication and relatively high cost of encapsulation methods have made them impractical to use on a large scale in the construction industry.

So far, the most suitable carrier for bacteria has not been found, creating the need to develop better techniques to carry bacteria. In this study, the feasibility of using cellulose fiber as a bacteria-carrier is investigated.

1.3 Use of cellulose fibers in autogenous healing of concrete and as a bacteria-carrier in self-healing mortar:

Van Tittelboom and Belie [23] explained in their study that self-healing in concrete is more effective when the crack width is restricted (Figure 1A), water is available in the cracks (Figure 1B), and crystallization of self-sealing products takes place (Figure 1C).

The author hypothesizes that cellulose fiber can assist in improving all three mechanisms noted above (A, B, C). For A, cellulose fibers can limit crack width in the plastic shrinkage phase [27] and can reduce the cracking by 85% more than normal concrete [28, 29]. Cellulose fibers have a high water absorption of 85% [30], thus improving internal curing and assisting in mechanism B. Finally, since cellulose fibers have high alkali resistance

[31], they can protect bacteria from highly alkaline concrete environment and would provide enriched sites to bacteria for MICP in case of self-healing mortar and they also work as a water reservoir which leads to the crystallization of cement hydration products due to continuous hydration, required for autogenous healing of concrete.

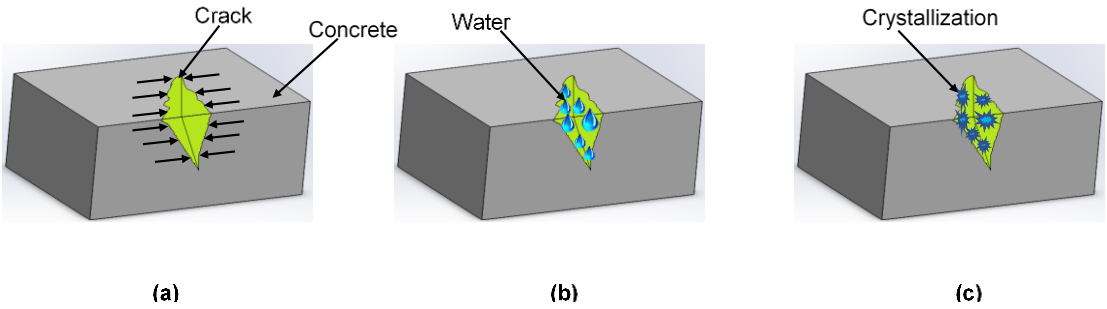

Figure 1. Conditions to improve self-healing: (a) Restriction of crack width; (b) Availability of water; (c) Crystallization. (Concept adopted from Van Tittleboom and Belie [23])

1.4 Working of self-healing mortar using cellulose fiber as a bacteria-carrier

The working mechanism of cellulose fiber based bacterial mortar is shown in Figure 2. When the mortar is not cracked the bacteria remain dormant inside the fibers distributed throughout the matrix. After the cracks appeared, the cellulose fibers containing bacteria act as a bridge between the cracks, outside oxygen and water can enter the mortar through cracks, activating the bacteria. The activated bacteria work on the nutrients present in the mortar or in curing water and results in the MICP to seal the cracks gradually.

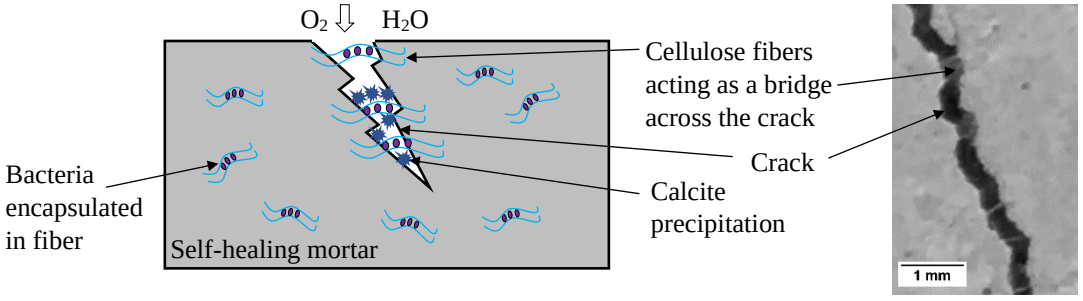

Figure 2: The working mechanism of self-healing mortar using cellulose fiber as a bacteria-carrier

In self-healing mortar the advantages of using cellulose fiber are:

- The high porosity of fibers helps to provide space for the growth of bacteria. Additionally, the porosity of fiber also helps to absorb water and oxygen, which can be utilized by bacteria at the time of MICP.
- Fibers works as a bridge across the crack surfaces result in an increase in the availability of bacteria for the self-healing inside the crack.
- Fibers help to reduce brittleness and the microcracking in the mortar leads to an increase in the efficiency of self-healing.
- Encapsulation of bacteria can be done by just submerging fibers into bacterial suspension to make them saturate, which is a very easy and practical method.
- Cellulose fibers are also suitable for concrete ready-mix plants [29] which makes them easy to use as a bacteria-carrier in the small to large scale concrete construction.

In addition, cellulose fibers in concrete increase the freeze-thaw durability [32] and provide a nice finished surface [33]. So, it is hypothesized that the use of cellulose fiber as a bacteria-carrier would resist the crack formation as well as improve the self-healing and autogenous healing of the cement mortar and concrete respectively

1.5 Objectives

Two types of materials were analyzed in this study; CeFRC and bacteria-based self-healing mortar. The fundamental goal of this thesis is to experimentally investigate the self-healing, durability and strength properties of CeFRC, and the feasibility of using cellulose fiber as a bacteria-carrier in self-healing mortar.

Objective I: Study the effect of fiber addition on the strength of self-healing mortar.

Objective II: Compare the cost of cellulose fiber with other bacteria carriers.

Objective III: Examine the effect of fibers on autogenous self-healing of concrete.

Objective IV: Study the water permeability and mechanical properties of CeFRC.

Objective V: Investigate the efficiency of self-healing mortar using cellulose fiber as a bacteria-carrier.

1.6 Scope of Work

The experiments were conducted on the CeFRC and self-healing mortar to meet the required objectives of the study. First, the influence of cellulose fiber addition on autogenous self-healing and water permeability properties of concrete were determined. After that cellulose fibers and bacteria were used together to investigate the feasibility of cellulose fiber as a novel bacteria-carrier for self healing mortar. Figure 3 shows the scope of work of the study in the form of a flow chart.

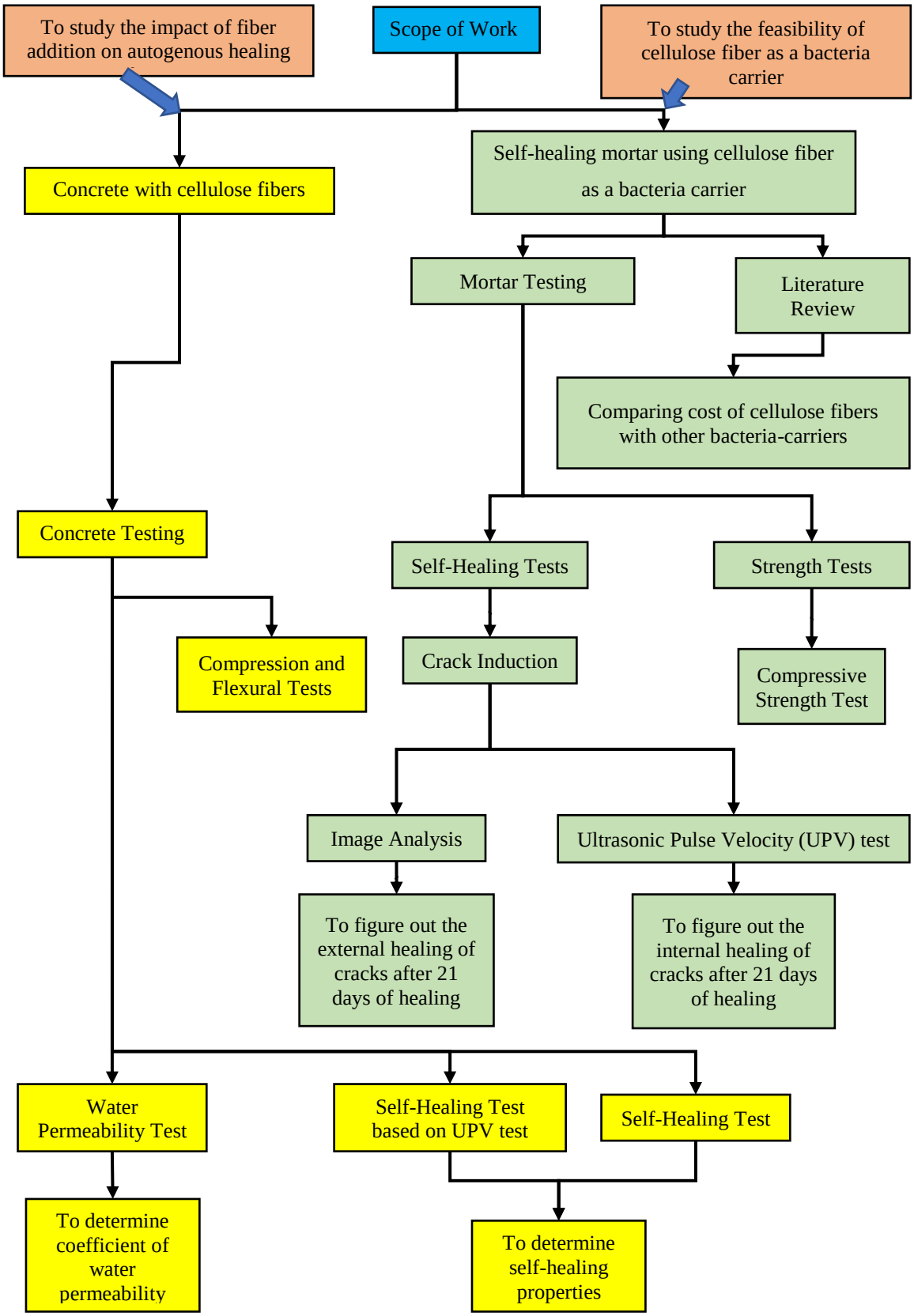

Figure 3: Scope of Work

1.7 Publications

1.7.1 Journal papers

H. Singh, R. Gupta, "Use of cellulose fiber as reinforcement and bacteria-carrier in self-healing mortar," *Journal of Building Engineering*, {Under Peer Review, Submitted on 22 July 2019}

H. Singh, R. Gupta, "Influence of cellulose fiber addition on self-healing and water permeability of concrete," *Case Studies in Construction Materials*, {Submitted on 03 September 2019}

1.7.2 Conference papers

H. Singh, R. Gupta, "Strength recovery and crack healing of self-healing cement mortar containing cellulose fibers and bacteria," in *1st International Conference on New Horizons in Green Civil Engineering*, Victoria, 2018.

1.8 Layout of Report

A brief overview of each chapter of the report has been explained below:

Chapter 1 Introduction need of study, objectives, and scope of the study has been explained in this chapter.

Chapter 2 discusses the properties of different materials used in experimental work. Mix design procedures for various mixes and different testing procedures used in the experimental program has been discussed.

Chapter 3 Various test results for CeFRC are presented and discussed which include the self-healing tests, water permeability test, flexural, and compressive strength test results.

Chapter 4 Various test results for self-healing mortar using cellulose fiber as a bacteria-carrier are presented and discussed. Which includes the self-healing tests, and compressive strength test results.

Chapter 5 Consists of concluding remarks and future scope of work based on work carried out in this research.

Chapter 2. Experimental Programme

2.1. Material Properties

The following sections specify the types and associated properties of different materials used in the preparation of concrete and mortar:

2.1.1. Cement

General use Type GU Ordinary Portland Cement (OPC), which also meets the requirements of type-I and type-II cement as per ASTM C150 [34] specifications, was used in the making of concrete and mortar samples.

2.1.2. Aggregates

Aggregates used for the preparation of concrete and mortar were obtained from the Sechelt pit in B.C. Coarse and fine aggregates had a relative dry density of 2.695 and 2.651 respectively, related absorption ratio of 0.69% and 0.79% respectively. The maximum size of coarse and fine aggregates was 12.5 mm and 4.75 mm respectively.

2.1.3. Cellulose Fiber

Fibers used in this study were obtained from Solomon colours, INC. These fibers are a special type of natural cellulose fibers called UltraFiber 500 made from Slash pines and Loblolly in North America. As per the manufacturer's declaration, UltraFiber 500 is an alkali resistant cellulose based microfibers used for secondary reinforcement, provide crack control and have better hydration and bonding properties [35]. A close-up view of cellulose fibers is shown in Figure 4.

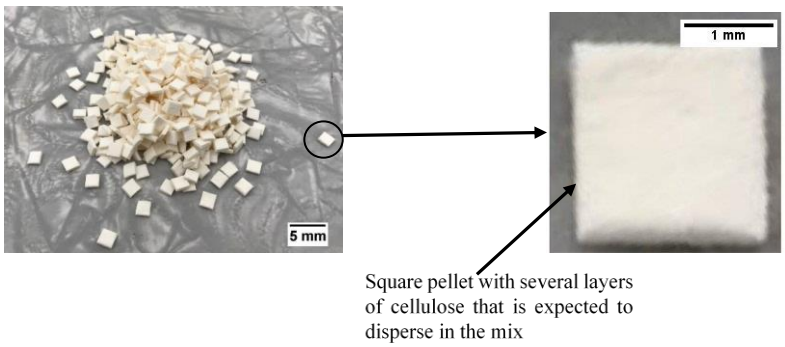

Figure 4: Micro cellulose fibers

Use of these fibers in concrete also supports the purpose of sustainability as they come from natural renewable resources. Apart from this, high surface area and close spacing of cellulose fibers make them quite effective in the suppression and stabilization of microcracks in the concrete matrix [36]. General properties of cellulose fibers are presented in Table 2.

Table 2: General Properties of UltraFiber 500 [37]

Name of Fiber	UltraFiber 500
Material Type	High Alkali Resistant, natural cellulose fibers
Average Length	2.1 mm
Average Denier	2.5 g/9,000m
Average Diameter	0.00063 inch
Count, fiber/lb	720,000,000
Density	1.10 g/cm^3
Surface Area	25,000 cm^2/g
Tensile Strength	750 N/mm^2
Average Elastic Modulus	8500 N/mm^2
Water Absorption	Up to 85% of fiber weight [30]

Steel and glass fibers have the more tensile strength than cellulose fibers, 1100 N/mm^2 and 2450 N/mm^2 respectively [38]. However, corrosion of steel fiber take place in concrete matrix when comes in contact with water and glass fibers become fragile with age. Cellulose fibers are high alkali resistant and also have more tensile strength and water absorbtion as compared to polypropylene (tensile Strength = 300-400 N/mm^2 [38] and water absorption 0.3% [39]) fibers.

2.1.4. Bacteria:

Bacillus subtilis is a gram-positive bacterium, also known as the *hay bacillus* or *grass bacillus*, found in the soil and the gastrointestinal tract of human and ruminants [40]. The *Bacillus subtilis* strain 168, cultured and grown at the microbiology laboratory of the University of Victoria, was used in this study.

The medium composition used for the growth of bacterial culture was Peptone 5 g/ Litre, NaCl 5 g/ Litre and Yeast Extract 3 g/ Litre. The medium was first sterilized by autoclaving

at 121°C for 20 minutes. Then, the culture was incubated at 35°C with shaking at 200 rpm for 72 hours.

Microbial enumeration method was used to calculate the number of bacteria per ml of the solution. The serial dilutions plating and counting of live bacteria were done to determine the number of bacteria per ml of the solution. The 10 µL of four bacteria dilution samples (10^{-3},10^{-5}, 10^{-7}, 10^{-9}) were incubated on tryptone soya agar plates (see Figure 5) and the number of colony forming units (CFUs) was counted.

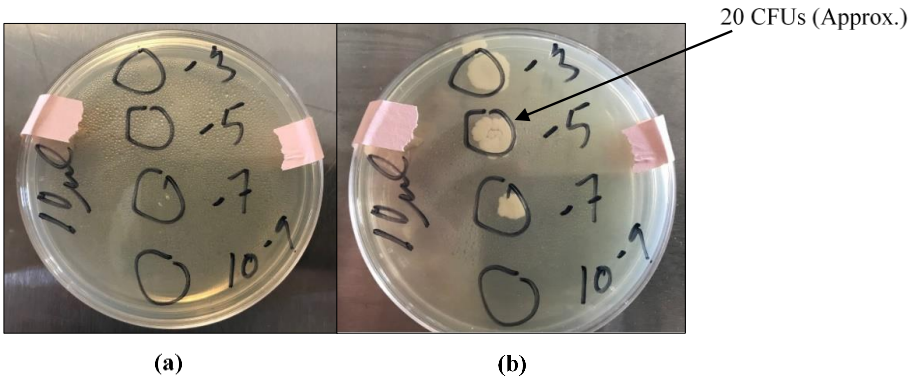

Figure 5: Bacteria colony forming units; (a) Plating of bacteria dilutions, (b) CFUs counting.

Dilution 10^{-5} had the most consistent number of CFUs for different plates. So, 10^{-5} dilution was used to calculate the number of bacteria/ml.

$$\frac{\text{Number of Colony Forming Units}}{\text{Volume plated (mL) x total dilution used}} \rightarrow \frac{20}{0.01 \text{ mL x } 10^{-5}} \rightarrow 2\text{x}10^{8} \text{ Bacteria/ml}$$

Hence the bacteria concentration was 2 x 10^{8} bacteria per ml of the bacterial suspension.

2.1.5. Calcium Lactate:

The calcium lactate is used as a nutrient for bacteria because it does not interfere with the setting time of the concrete. It is a white crystalline salt with chemical formula $C_6H_{10}CaO_6$. Calcium lactate for this study was purchased from iChemical Technology USA Inc. Table 3 shows the general properties of calcium lactate.

Table 3: General properties of calcium lactate [41]

Physical State	Powder
Colour	White
Boiling Point	227.6 °C at 760 mm Hg
Flash Point	109.9 ºC
Molecular Formula	$C_6H_{10}CaO_6$
Molecular Weight	218.22

2.2. Mix Design

2.2.1. Concrete Mix Design:

The cement/sand ratio and water/cement ratio used was 0.41 and 0.53 respectively in all types of concrete mixes, which represents a mix with a target strength of 32 MPa, normally used in the field. In this study, 0.5% volume fraction of cellulose fibers was used to increase the dispersion of fibers throughout the matrix. Moreover, Banthia et al. also used the same volume fraction of cellulose fibers in their study on fiber reinforced concrete for flexural and direct shear tests [42]. Two types of mixes were formulated:

1. **Cxx:** Control concrete.
2. **0.5Cxx:** Cellulose fiber concrete with fiber volume fraction equal to 0.5%.

Where C and xx refer to concrete and sample number respectively. The decimal fraction indicates the volume fraction of cellulose fibers used in the concrete. Mix proportion used for concrete is presented in Table 4.

Table 4: Mix proportions for concrete

Material	Quantities	Units
Cement	340	
Aggregates	1120	
Sand	820	kg/m^3
Water	181	
Cellulose Fibers 0% and 0.5%	0 and 5.5	

2.2.2. Mortar Mix Design:

The cement/sand and water/cement ratios for mortar mix design were selected as 0.33 and 0.5 respectively, which represents a typical mix used in the field with a target strength of 32 MPa. Singh and Gupta [13], used the 0.25% volume fraction of fibers to encapsulate

bacteria in their study and no visible healing of cracks was observed by them for this volume fraction of fibers. In this study, 0.5% volume fraction of cellulose fibers was used to increase the fibers available for bacteria encapsulation. Four types of mixes were formulated:

1. **CMxx:** Control mortar.
2. **CO.5Mxx:** Control mortar with cellulose fibers equal to 0.5% of the volume fraction.
3. **BL0.5Mxx:** Mortar with *bacillus subtilis* equal to 1.3 x 10^7 bacteria/cm^3 of cement mortar encapsulated in cellulose fibers (0.5% of the volume of mortar) and calcium lactate equal to 4.5% of cement weight.
4. **B0.5Mxx:** Mortar with *bacillus subtilis* equal to 1.3 x 10^7 bacteria/cm^3 of cement mortar encapsulated in cellulose fibers (0.5% of the volume of mortar) and cured in water containing calcium lactate.

Where C, M, B, L, and xx refers to control, mortar, bacteria, calcium lactate, and sample number respectively. The decimal fraction indicates the percentage volume of cellulose fibers in cement mortar. Mix proportion used for mortar is represented in Table 5.

Table 5: Mix proportions for cement mortar

Material	Quantities	Units and Remarks
Cement	736	kg/m^3
Sand	2207	
Water	368	
Cellulose Fibers 0% and 0.5%	0 and 5.5	
Bacterial Solution (2x10^8 bacteria/ml)	0.065	ml/cm^3 results in 1.3 x 10^7 bacteria/cm^3 of cement mortar
Calcium Lactate (4.5% of cement weight)	33.12	kg/m^3

2.2.2.1. Encapsulation of Bacteria in Cellulose Fiber

The required quantity of cellulose fibers was kept soaked in the required quantity of bacterial solution for BL0.5Mxx and B0.5Mxx mixes for 24 hours (see Figure 6). The amount of bacteria solution absorbed by fibers is 85% of the weight of fibers, results in 9.3 x 10^5 encapsulated bacteria/cm^3 of mortar.

Figure 6: Bacteria encapsulated in cellulose fibers

2.3. Mixing, Curing and Setting Procedure for Concrete

For each mixture, in total twelve cylinders of size Φ100 x 200 mm, three beams of size 355 x 101 x 101 mm and three cylinders of size Φ150 x 175 mm for water permeability test were prepared as per the recommendations of ASTM C192 [43]. Ingredients for both mixes were batched out as per the final volume of concrete required by using an electronic weighing balance. For CeFRC, the mixing procedure was started by first soaking cellulose fibers in 20% of total mix water for 15 minutes. This was done to prepare a slurry paste of cellulose fibers to improve the uniform mixing of fibers with other ingredients. After the formation of a slurry, it was mixed with coarse aggregates for two minutes, once slurry was thoroughly mixed, remaining ingredients were added to the drum mixer and mixed for three minutes followed by two minutes rest and a two minutes final mixing. Once the uniform mix was achieved, a slump test was performed within 15 minutes as per ASTM C143 [44], afterward, the concrete was placed into desired molds.

To ensure sufficient compaction, removal of entrapped air and to avoid honeycomb structure, filled molds were placed on a vibrating table for 30 seconds. After compaction, molds were covered with a plastic sheet and placed at room temperature for the next 24 hours. Demolding was carried out after 24 hours and samples were placed in a curing chamber maintained at 23 ± 2º C. Table 6 summarizes the specimens' type and quantity as well as curing age used for different test methods.

Table 6: Details of specimens used in different test methods

Test method	Number of specimens	Type of specimen	Curing Age (d)	Standard
Compressive Strength	3	Cylinder (Φ100 x 200 mm)	14	ASTM C39
Compressive Strength	3	Cylinder (Φ100 x 200 mm)	28	ASTM C39
flexural Strength	3	Beam (355 x 101 x 101 mm)	28	ASTM C293
Water Permeability	6	Cylinder (Φ150 x 175 mm)	28	DIN 1048
Self-healing	3	Cylinder (Φ100 x 200 mm)	2 (Dry Cured)	Patented test [45]
UPV	3	Cylinder (Φ100 x 200 mm)	28	C597

2.4. Mixing, Curing and Setting Procedure for Mortar

Ingredients for different mixes were batched out as per the final volume of mortar required by using an electronic weighing balance. A homogeneous mixture of cellulose fibers was achieved by preparing a fiber mixture in bacterial solution, followed by mixing in the sand for a minute using a table mixer. Afterward, required cement and water quantities were added to the paste, calcium lactate was added for BL0.5Mxx mix and mixed for another minute. The amount of water used for each mix was adjusted for the amount of bacterial solution used. Once the uniform mix was achieved, the mortar was placed into cube molds of size 50 mm, shown in Figure 7. To ensure maximum compaction and removal of entrapped air, manual compaction was done using a tamping rod. The mortar was placed in molds in two equal layers and each layer was tamped 25 times. After compaction, molds were covered with a plastic sheet and placed at room temperature for the next 24 hours. Demolding was carried out after 24 hours and samples were placed in a water tub maintained at 23 ± 2° C after appropriate labeling based on the mix design. The bacterial mix without calcium lactate (B0.5Mxx) was cured in water containing calcium lactate. The amount of calcium lactate added to curing water was equal to 4.5% of the cement content of the cubes cured in that water.

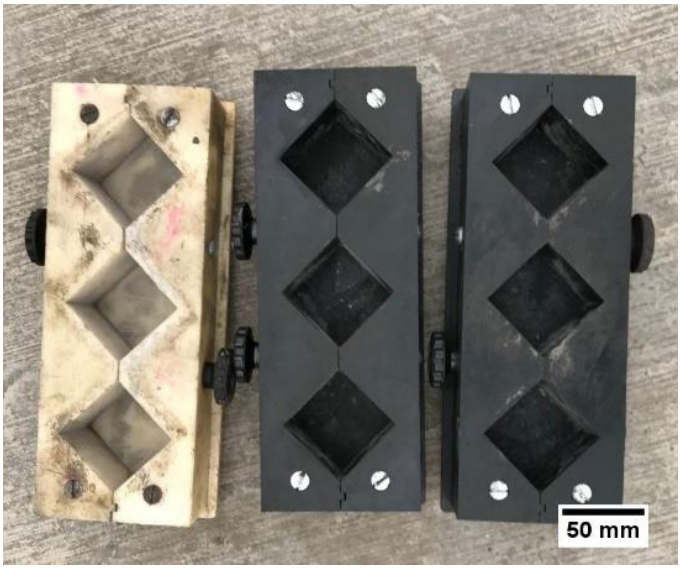

Figure 7: Cube molds

Figure 8 shows the preparation of self-healing mortar by using cellulose fiber as a bacteria-carrier. The cellulose fibers were kept soaked in bacterial suspension for 24 hours to encapsulate bacteria. Bacterial nutrient calcium lactate was mixed with mortar ingredients for BL0.5Mxx mix and mixed in curing water for B0.5Mxx specimens.

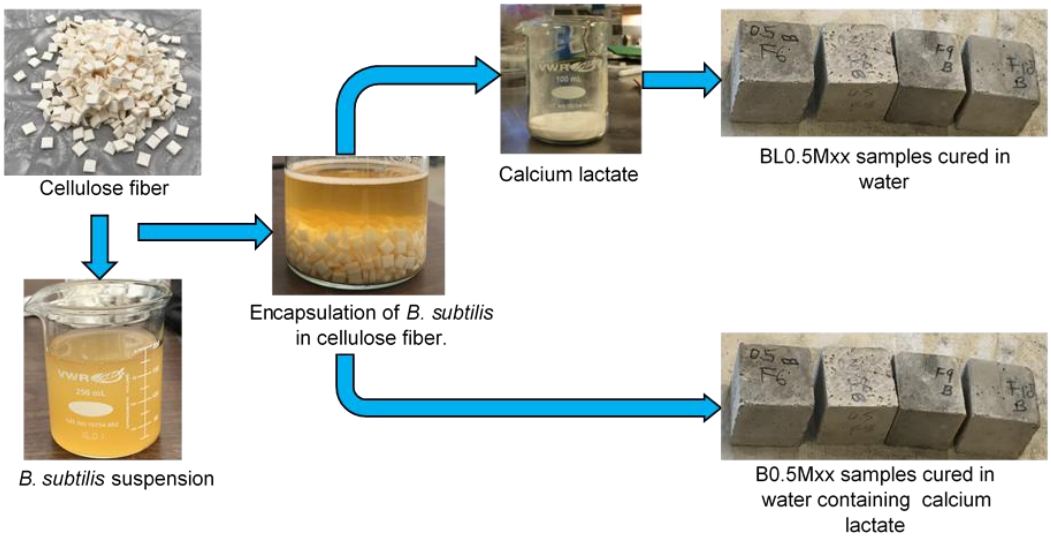

Figure 8: Preparation of self-healing mortar specimens using cellulose fiber as a carrier for bacteria

Fifteen mortar cubes of size 50 mm were prepared for each mix (CMxx, C0.5Mxx, BL0.5Mxx and B0.5Mxx), resulting in a total of 60 specimens. Table 7 summarizes the specimens' type and quantity as well as curing age used in different test methods.

Table 7: Type, number and curing age of mortar specimens used in different test methods

Test method	Number of specimen	Type of specimen	Curing Age
UPV and Image Analysis	5	Cube (50 mm)	14 days
UPV and Image Analysis	5	Cube (50 mm)	28 days
Compressive Strength	5	Cube (50 mm)	28 days

The cubes of size 50 mm were chosen as the only limited amount of bacteria could be cultured in the laboratory.

2.5. Testing Procedure for Concrete

Various types of tests were conducted to investigate the self-healing and strength characteristics of both concrete mixes. The UPV and self-healing tests were performed to evaluate the self-healing efficiency of concrete. Compression and flexural tests were used to determine the strength characteristics of the concrete mixes. Water permeability test was performed to determine the coefficient of permeability of concrete.

2.5.1. Compression Test for Concrete:

After 14 and 28 days of curing, to determine the compressive strength of concrete, three cylinders from each mix were tested as per the procedure defined in ASTM C39 [46]. Uniaxial compression testing machine was used to test the cylinders and the peak load was recorded at the time of failure. The loading rate was used within the range specified by the standard. 14 and 28 day cured samples were used to investigate the change in compressive strength with curing time.

2.5.2. Flexural Test for Concrete:

Prismatic beams of size 355 x 101 x 101 mm were tested at 28 days by using center point loading test as per ASTM C293-16 [47], to determine the flexural strength of both concrete mixes. A span of 304.8 mm (12”) was used over the supports. The universal testing machine was used to test the beams for flexural and peak load was recorded at the point of failure. Figure 9 shows the arrangement for the flexural test of concrete using center point loading method.

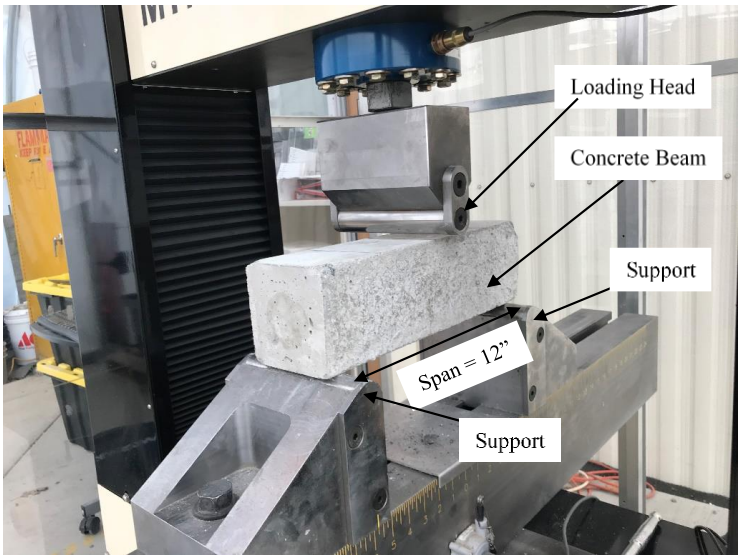

Figure 9: Center-point loading arrangement for the flexural test

The modulus of rupture was calculated using the equation (1) below:

$$R = \frac{3PL}{2bd^2} \quad (1)$$

Where R = modulus of rupture (MPa), P = maximum applied load indicated by the testing machine (N), L = span length (mm), b = average width of the specimen at the fracture (mm), d = average depth of specimen at the fracture (mm). By substituting appropriate values, equation (1) reduces to $R = 0.000435P$.

2.5.3. Water Permeability Test for Concrete:

Figure 10 shows the testing arrangement used for the permeability test. The test was performed for all mixes using DIN-1048-Part 5 standard [48]. Six specimens from each mix were subjected to 0.5 MPa water pressure for three days (72 hours). Prior to testing, the surface of the sample subjected to water pressure was roughened by wire brushing as recommended by the standard. The specimens were mounted on the rubber gasket with a 100 mm diameter to avoid any leakage during testing. After the testing was finished, the samples were split into two halves from the middle, perpendicular to the water injected surface by using the compression testing machine. The water penetration depth was marked for broken samples and measured.

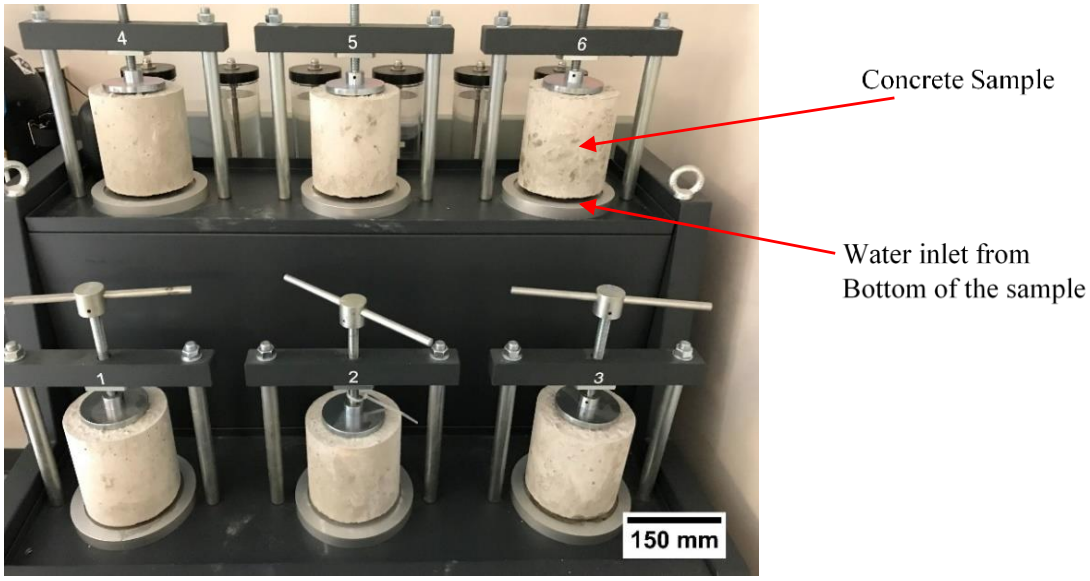

Figure 10: Permeability test arrangement

Assuming the flow of water through concrete pores is laminar and stationary, the coefficient of permeability can be calculated using Darcy's law [49] as follows:

$$\frac{dx}{dt} = K_w \frac{h}{x} \quad (2)$$

Where x is the depth of water penetration in meters, t is the time for the test in sec, h is the water pressure head and K_w is the water permeability coefficient. The K_w can be figured out by integrating equation (2) to yield equation (3):

$$K_w = \frac{x_t^2}{2ht} \quad (3)$$

Where x_t is the penetration depth at time t. Since the water flow is unsteady and associated with the sorptivity, it is more reasonable to use average depth instead of maximum penetration depth to calculate K_w [49, 50]. The x_{avg} was calculated by first measuring the wet area (A_w) and maximum width (W_{max}) of the wetted region by using *imageJ* software as shown in Figure 11. The x_{avg} was calculated as an average of A_w divided by w_{max} for each half of the tested sample.

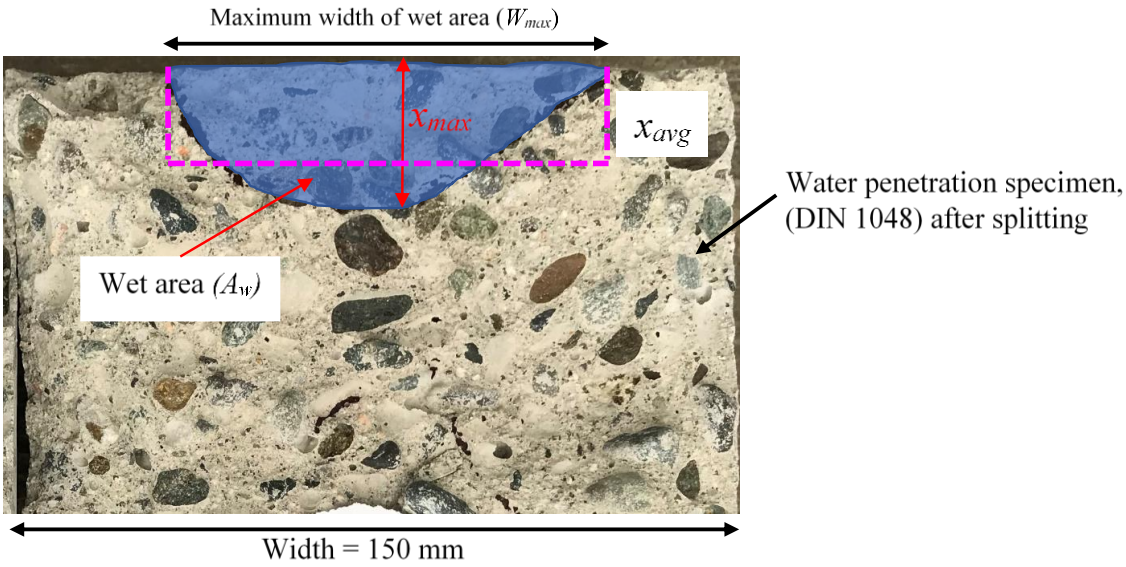

Figure 11: Method to calculate the average width (x_{avg}) in the wetted region

2.5.4. Ultrasonic Pulse Velocity (UPV) Test for Concrete:

The UPV test is a very sensitive indicator of the presence of damage (cracks/flaws) in concrete when performed under laboratory conditions [51]. Ariffin et al. [52], Bahrin et al. [53] and Sarkar et al. [54] also used the UPV test to evaluate the self-healing performance of concrete. The UPV test was performed on samples as per C597-16 [55]. The longitudinal stress wave is propagated through the concrete samples and time required to travel the wave across the diameter of the cylinder was recorded. The travel time of the wave varies as a function of the density of the material, allowing the estimation of the discontinuities in the samples. The specimens prepared to monitor self-healing using UPV were pre-cracked after 28 days of curing. Cracks were induced in the cylinders by using a standard crack inducing jig (SCIJ) [45] shown in Figure 12. This jig uses the V shaped cutting edges that act as stress concentrators. The cylinder was assembled inside the jig and the compression machine was used to subject compressive loading till visible cracks appeared on the surface of the cylinder. The pre-cracked specimens were allowed to cure in water to allow any self-healing.

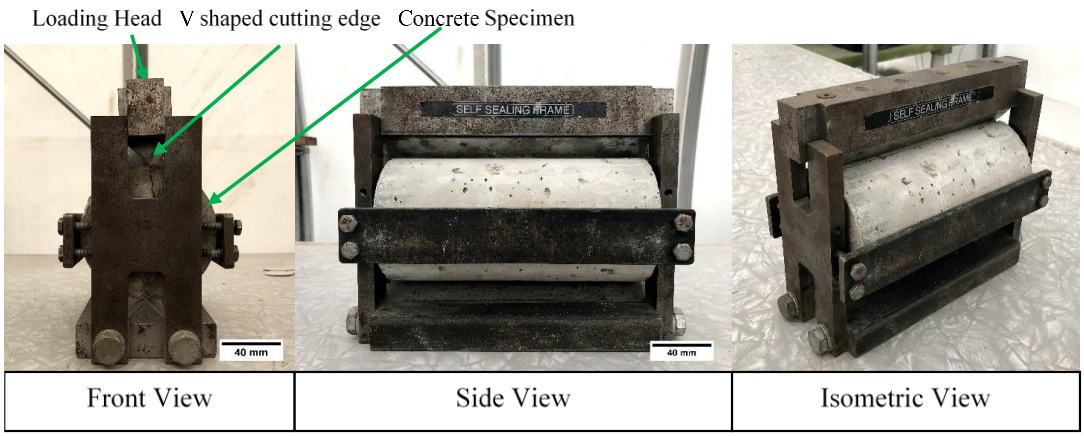

Figure 12: Crack Inducing Mechanism for Concrete Cylinders

The UPV test was performed on the uncracked and pre-cracked samples at the age of 28 days, followed by 21 days of healing. Figure 13 and Figure 14 shows the arrangement and sequence for the UPV test on concrete cylinders respectively. The device consists of two transducers one to transmit the ultrasonic wave and the other to receive it. Both transducers were connected with the surface of the cylinder and time required to travel the sound wave perpendicular to the crack direction (across the crack) as shown in Figure 14 was recorded with a precision of at least 0.1 µs. The coupling gel was applied on the surface to get a better contact area, required for accurate results. The test was performed at a frequency of 150 kHz. The velocity of the ultrasonic wave was calculated using the formula V = D/T, where D = diameter of the sample, 100 mm and T = time required to travel the distance, D.

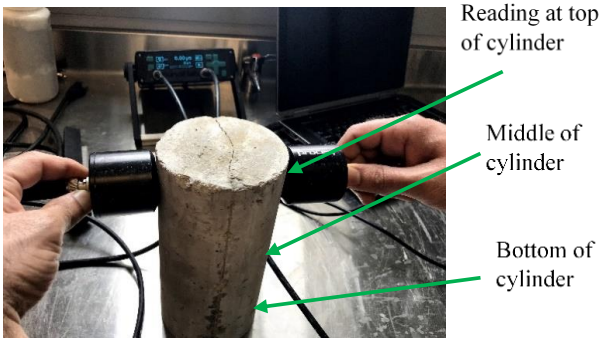

Figure 13: UPV Test Arrangement for Concrete

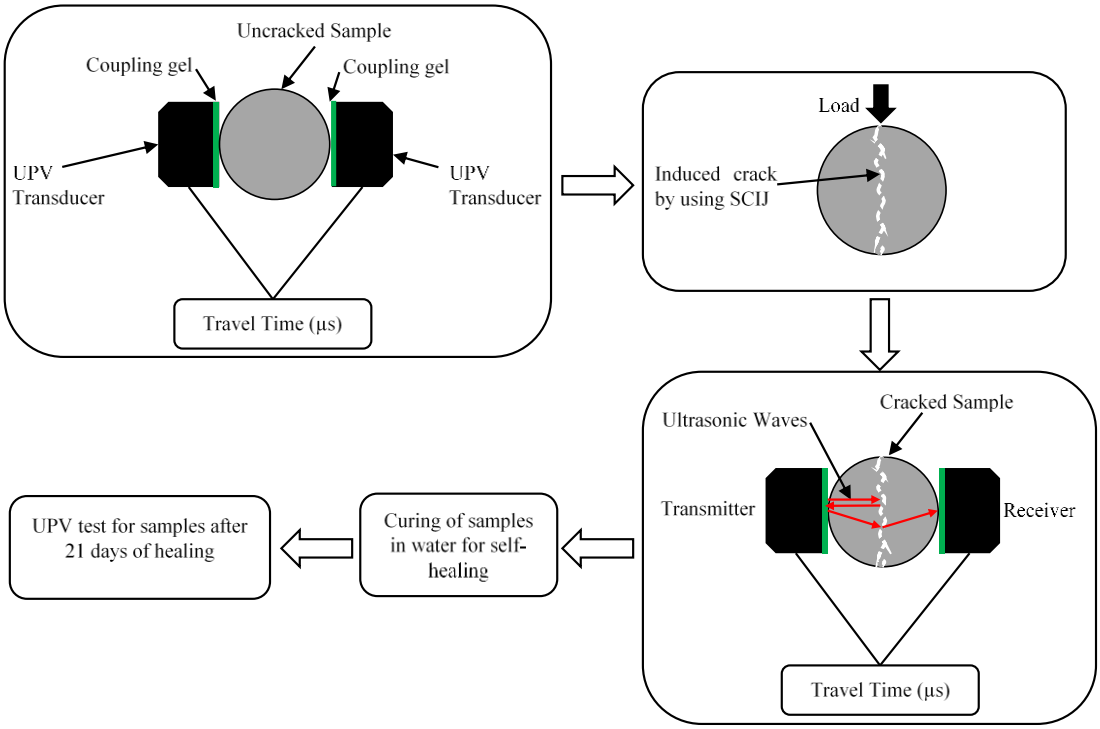

Figure 14: Sequence of UPV test to evaluate self-healing efficiency of concrete cylinders

2.5.5. Self-healing Test for Concrete

The self-healing test was performed by using the innovative technique developed by Gupta et. al [45]. The cylinders of Φ100 x 200 mm size were cracked using SCIJ [45]. Pejman et. al [50] also used the same method to evaluate the self-healing efficiency of concrete cylinders. The cylinders were cured in ambient temperature prior to cracking. After cracking, surface crack width of each cylinder was measured on top and bottom of the surfaces by using optical crack-detection-microscope at six equal distance points along the crack: three along the top face and three along the bottom face. All readings were averaged to calculate the average width of the crack for a cylinder. The cracked cylinders were inserted into special rubber sleeves and sealed using silicon sealant and epoxy resin to make sure water only passes through the crack during the self-healing test. The one end of the cylinder with rubber sleeves was exposed to a constant water head of 1.7 m. The flow of water through the crack of the cylinder was collected in a water container and measured at frequent intervals. Figure 15 shows the self-healing test arrangement for concrete cylinders.

Figure 15: Self-healing test arrangement for concrete cylinders.

2.6. Testing Procedures for Mortar

Three types of tests were conducted to investigate the self-healing and strength performance of all mortar mixes. The self-healing tests were performed to evaluate the self-healing efficiency and a compression test was used to determine the strength properties of the mortar mixes.

2.6.1. Self-Healing Evaluation:

Two tests were performed to evaluate the self-healing efficiency of mortar mixes which are explained below.

2.6.1.1. Visual Inspection of Cracks:

The specimens prepared to monitor self-healing were pre-cracked after 14 and 28 days of curing. Cracks were induced in the cubes by using the standard crack inducing jig (SCIJ) [45], shown in Figure 16.

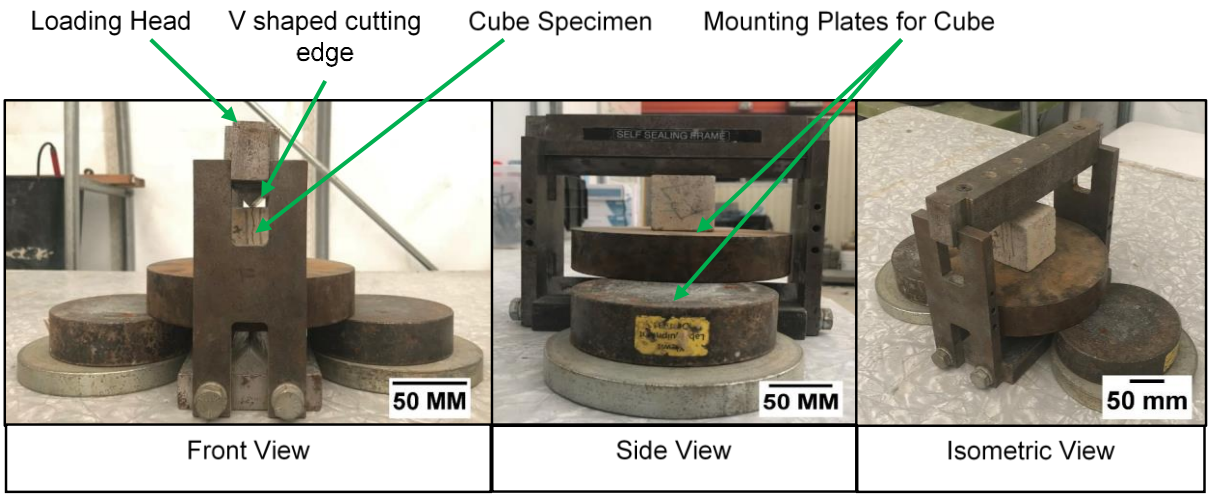

Figure 16: Crack Inducing Mechanism for Mortar Cubes

This jig uses the V-shaped cutting edges that act as stress concentrators. The cube was assembled inside the jig and the compression machine was used to subject compressive loading till visible cracks appeared on the surface of the cube. After inducing a crack, images of the cubes were taken and analyzed using a software *ImageJ* to determine the average width of the crack. The pre-cracked specimens were continued to cure in water to self-heal. After pre-cracking, images were taken after regular intervals of 7, 14 and 21 days. Pre-cracked images were compared with later days to see the evidence of any healing of cracks on the surface due to bacterial activity.

2.6.1.2. Ultrasonic Pulse Velocity (UPV) Test:

The UPV test was performed on samples as per C597-16 [55]. The longitudinal stress wave was propagated through the mortar samples and time required to travel the wave across the sample was recorded. Figure 17 and Figure 18 shows the sequence and arrangement for the UPV test respectively.

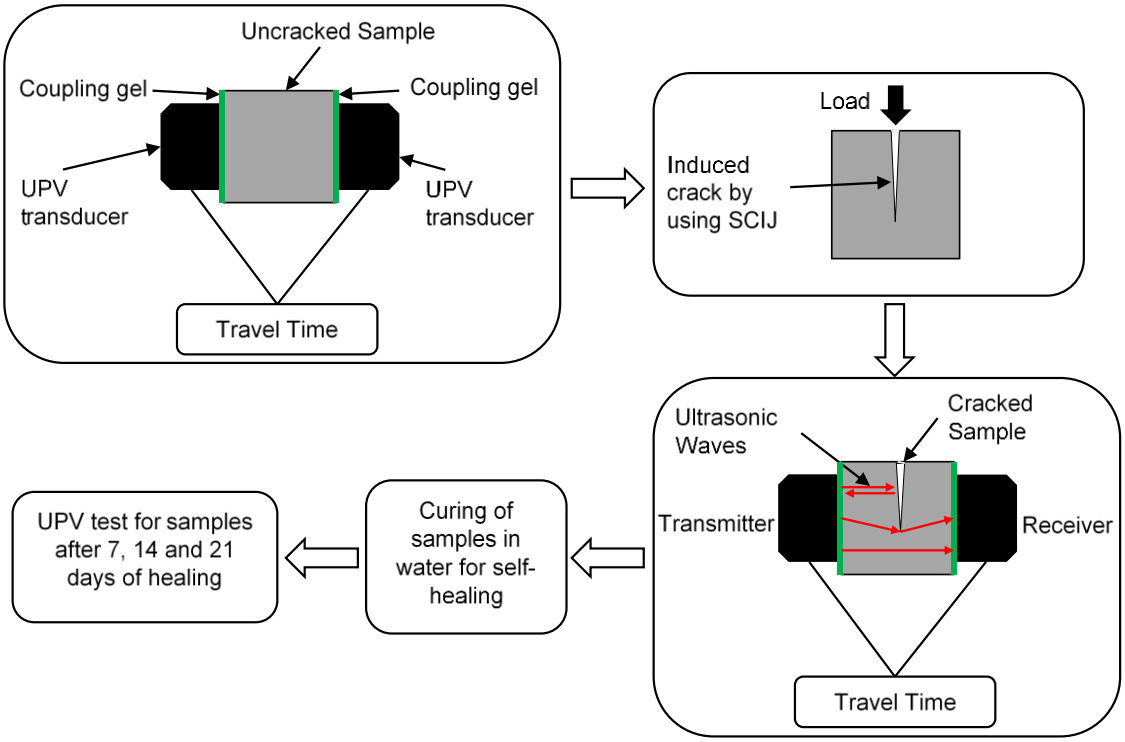

Figure 17: Sequence of UPV test to evaluate self-healing efficiency of mortar mixes

Figure 18: UPV test arrangement for mortar

Both transducers were connected with the surface of the mortar samples and time required to travel the sound wave across the sample was recorded with a precision of at least 0.1 µs. The coupling gel was applied on the surface and the test was performed at a frequency of 150 kHz. The velocity of the ultrasonic wave was calculated using the formula below:

V = D/T, D = dimension of sample, 50 mm, T = Time required to travel the distance, D.

The test was performed on the uncracked and pre-cracked samples at the age of 14 and 28 days, followed by 7, 14 and 21 days of healing. The 14 and 28 days pre-cracked samples were used to observe the impact of age of the mortar on self-healing performance.

2.6.2. Compression Test for Mortar:

Cubes were tested after 28 days of curing to determine the strength of mortar. Five cubes were tested for each type of mix to determine the average compressive strength. ASTM C579 [56] states the method to determine the compressive strength of cement mortar cubes of size 50 mm. Uniaxial compression testing machine was used to test the cubes and the peak load was recorded at the point of failure. The loading rate was used within the range specified by the standard.

Chapter 3. Results and Discussion for CeFRC

3.1. Slump and Compressive Strength

The slump values of 75 mm and 35 mm were observed for the Cxx and 0.5Cxx mix respectively. A 53.3% decrease in the slump was observed for 0.5Cxx when compared to Cxx. The decrease in the slump is due to the fact that cellulose fibers are hydrophilic and they tend to soak most of the water during mixing (about 85% of their weight).

Table 8 shows the average compressive strength (f'c) of each mix along with averages and standard deviation values for 14 and 28 days cured samples.

Table 8: Compressive strength test results for concrete

Mix Design	**14 days Compressive Strength (f'c) (MPa)**		**28 days Compressive Strength (f'c) (MPa)**		**Number of Samples for Standard Deviation (N)**
	Individual	Average ± STDV	Individual	Average ± STDV	
Cxx	47.62	48.11 ± 2.16	48.71	48.52 ± 0.9	3
	50.97		49.52		
	45.74		47.34		
0.5Cxx	30.96	30.12 ± 0.63	37.53	36.21 ± 0.99	3
	29.97		35.96		
	29.43		35.15		

The data in Table 8 were analyzed for the % change in compressive strength of CeFRC from control concrete. The % change in compressive strength for 14 and 28 days cured mixes is shown in Figure 19. A decrease in compressive strength of 37.39% and 25.59% is noticed with addition of 0.5% fibers after 14 and 28 days of curing respectively. The decrease in compressive strength is possibly attributed to loss of workability of concrete when 0.5% by volume cellulose fibers are added, which causes lower compaction of concrete samples. However, a lower reduction in compressive strength is observed for 28 days cured samples as compared to 14 days cured samples because at longer age cellulose fibers act as a water reservoir that helps to improve the hydration of unreacted cement particles by means of internal curing. This internal curing in fiber concrete somehow compensates for the loss of f'c.

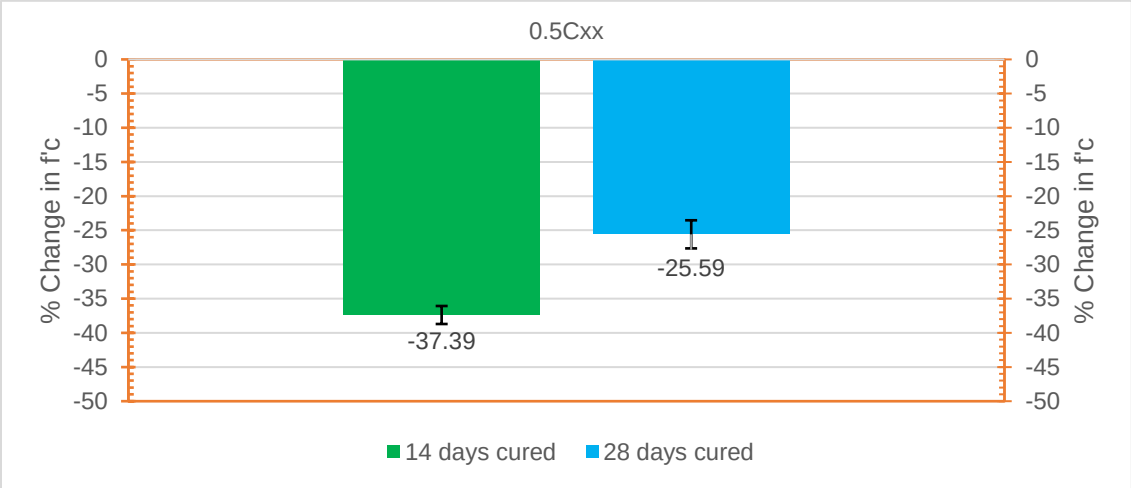

Figure 19: Effect of fiber addition on 14 and 28 days compressive strength

3.2. Flexural Strength

Table 9 shows the average flexural strength and corresponding maximum deflection for both mixes along with averages and standard deviation values for 28 days cured samples when tested in the form of beams under center point loading configuration.

Table 9: Flexural strength test results for concrete

Mix Design	28 days Flexural Strength (MPa)		28 days Maximum Mid-Span Deflection (mm)		Number of Samples for Standard Deviation (N)
	Individual	Average ± STDV	Individual	Average ± STDV	
Cxx	5.60 5.60 5.67	5.62 ± 0.03	1.33 1.43 1.76	1.51 ± 0.18	3
0.5Cxx	5.97 6.02 6.19	6.06 ± 0.09	1.767 2.22 2.56	2.18 ± 0.32	3

The data in Table 9 were analyzed for the % change in flexural strength of CeFRC from control concrete. Even though the f'c of this mix is lower the addition of cellulose fibers results in a 7.8% increase in flexural strength of normal concrete. A considerable increase in the maximum deflection at the time of failure is also observed, which indicates cellulose fiber has a good bond strength with the concrete matrix and able to transfer load under

tensile forces. Additionally, cellulose fiber has a significantly higher tensile strength (750 MPa) as compared to normal concrete (5 MPa), which also leads to an increase in flexural strength of concrete with the fiber addition.

3.3. Water Permeability Test

The permeability test was conducted on the samples based on DIN 1048. The penetration depth of samples that deviated more than 20% of the mean value of six samples were removed from the results. Figure 20 and Figure 21 shows the maximum and average penetration depths respectively for both concrete mixes. Hedegaard and Hansen [57] explained in their study that for all practical purposes concrete is considered as watertight when the maximum penetration depth is less than 50mm (2 inch). Both mixes indicated less than 50 mm maximum penetration depths which range from 24.11 mm to 28.33 mm for control mix and 17.57 mm to 21.54 mm for CeFRC. The addition of fibers significantly reduced the maximum and average water penetration depth for concrete. Figure 20 and Figure 21 exhibits that addition of fiber results in a 24% and 23.4% reduction in maximum and average water penetration depth respectively.

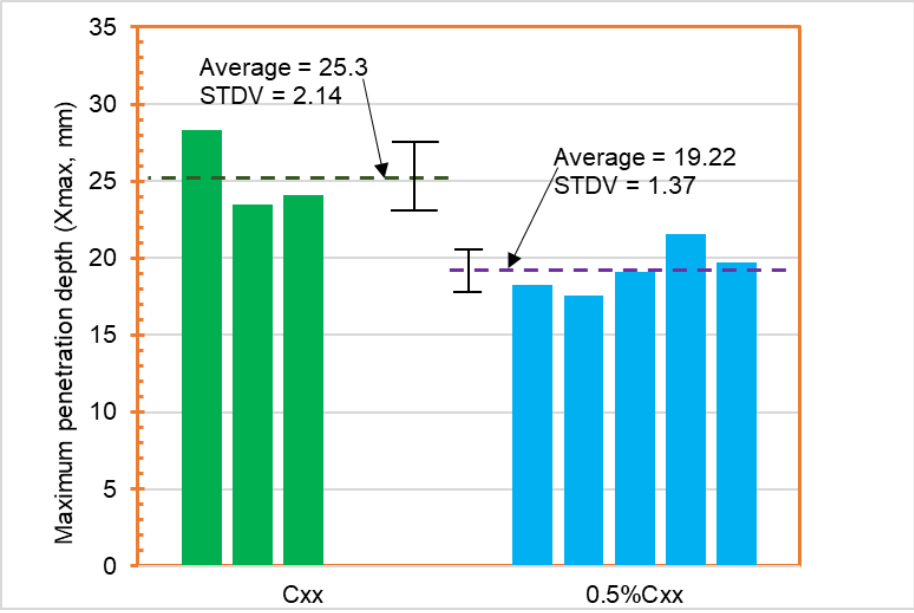

Figure 20: Maximum water penetration depth based on DIN 1048 test results

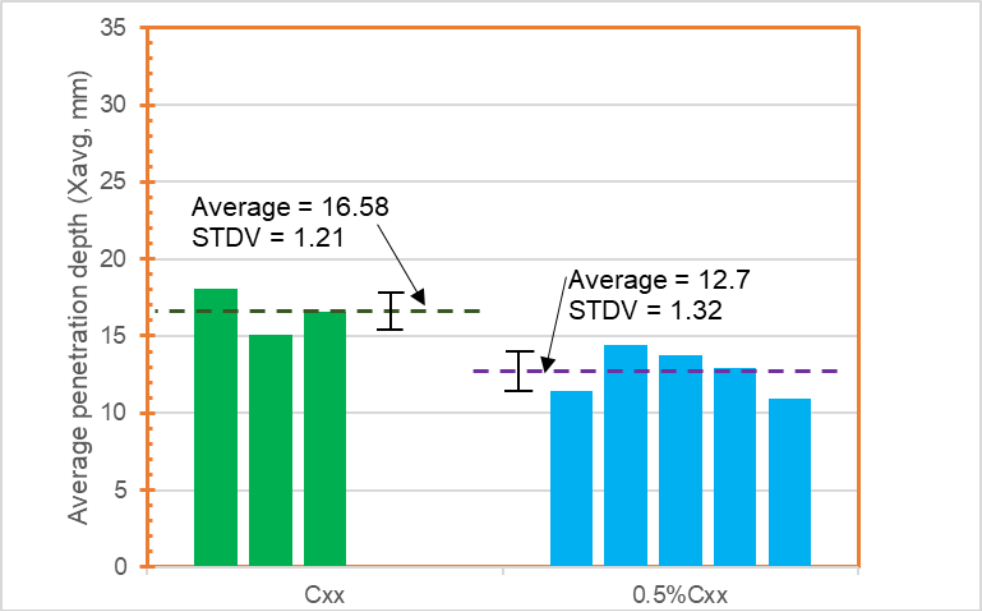

Figure 21: Average water penetration depth based on DIN 1048 test results

Also, when results are compared for maximum and average values of penetration depths, it was observed that standard deviation was lower for the average penetration depths, demonstrating average depth is more reliable than maximum depth.

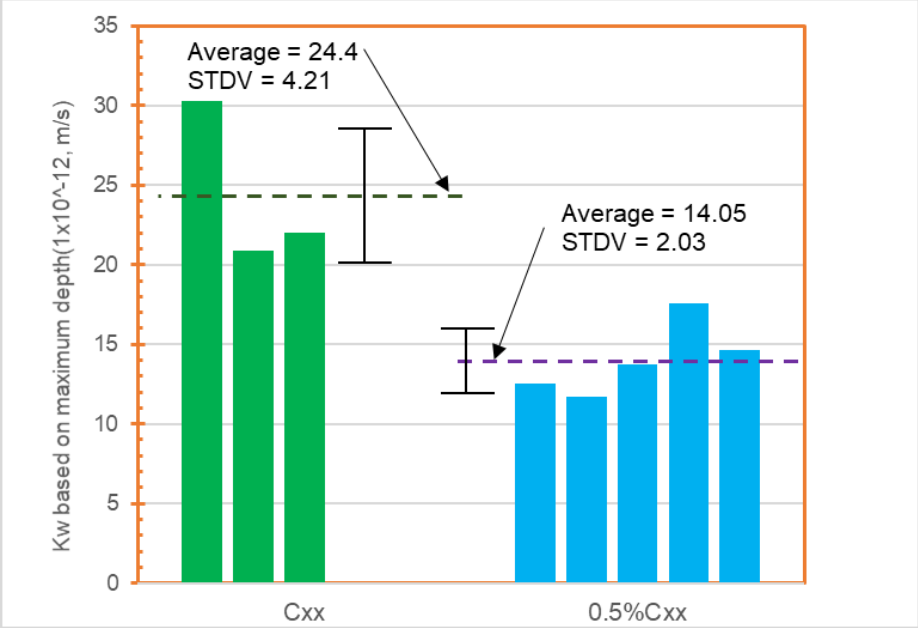

Figure 22: Coefficient of permeability using maximum depth based on DIN 1048 test results

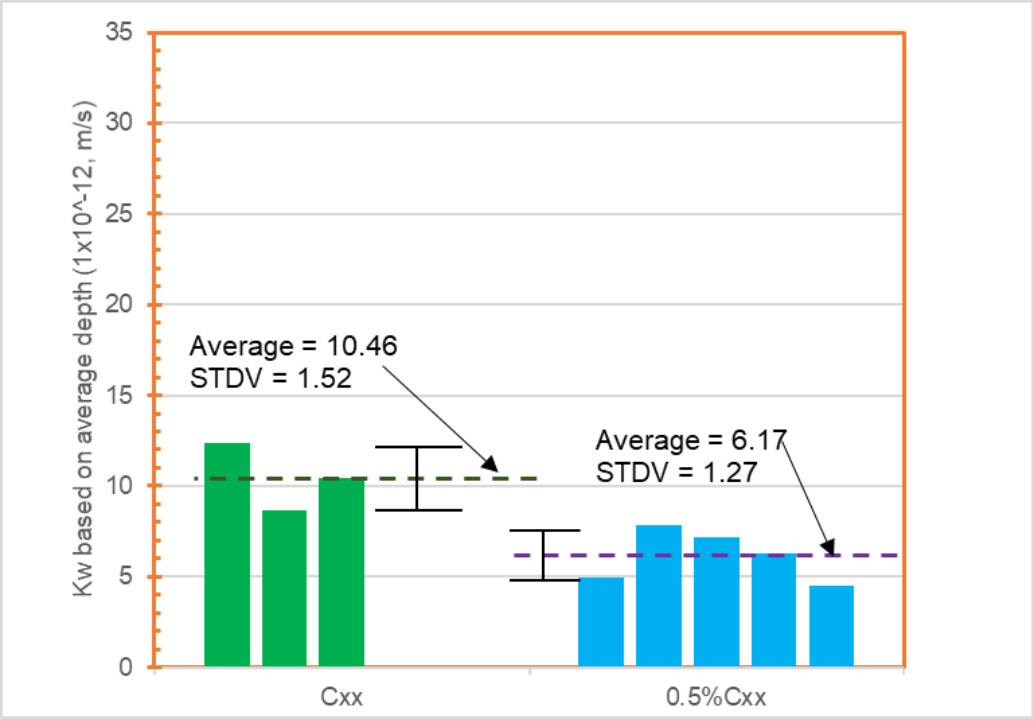

Figure 23: Coefficient of permeability using average depth based on DIN 1048 test results

Coefficient of permeability was also calculated using equation (3) based on DIN 1048 test results. Figure 22 and Figure 23 shows the permeability coefficient calculated based on maximum and average penetration depths respectively. Again, it can be observed that the addition of fibers resulted in a decrease in permeability coefficient by 42% and 41% calculated based on maximum and average penetration depths respectively. Considerable decrease in the penetration depths and coefficient of permeability indicates the effectiveness of cellulose fibers for waterproofing purposes in concrete.

3.4. Self- Healing Based on UPV Test

The self-healing potential of both concrete mixes was investigated by the UPV test. The UPV technique used to evaluate self-healing is the same as used by Ariffin et al. [52], Bahrin et al. [53] and Sarkar et al. [54]. The UPV time was recorded for uncracked, pre-cracked and 21 days healed concrete cylinders across the crack to study any interior healing of the cracks. For each sample, the test was performed at three locations of the cylinder; top, middle and bottom, and repeated at least three times for each location. Data were

presented as average ± standard deviation. Table 10 shows the UPV results for all concrete mixes uncracked and pre-cracked at 28 days.

Same as done by Zhong and Yao [58], the microstructure changes in concrete are inferred from the decrease of UPV by introducing a damaged degree defined as:

$$D = 1 - \frac{V_p}{V_0} \quad (4)$$

Where D is the damage degree of the concrete, V_p is UPV of the pre-cracked sample, and V_0 is the UPV of an uncracked sample. A self-healing ratio of concrete, SR, that incorporates UPV after 21 days of self-healing and pre-cracked sample can be introduced as:

$$SR = \frac{(V_{21} - V_p)}{V_p} \quad (5)$$

Where V_{21} is the UPV after 21 days of self-healing, and V_p is the UPV of the pre-cracked sample.

Mixes were compared based on the damaged degree instead of crack widths because induced cracks have varying widths and depths. Based on the availability and distribution of results, the data were averaged for damaged degree between 0.6 and 0.7 for both mixes. Figure 24 shows the curing days vs UPV relation and SR for 28 days aged pre-cracked samples for D between 0.6 and 0.7 for both mixes.

Zhong and Yao [58] explained in their study that the UPV of concrete is a combined effect of the matrix, microcracks, and macrocracks, which could be represented as:

$$V_c = \frac{1}{\frac{i_1}{V_1} + \frac{i_2}{V_2} + \frac{i_3}{V_3}} \quad (6)$$

Where V_c is the UPV of concrete, i_1, i_2, i_3 and V_1, V_2, V_3 are the volume fraction and UPV of the matrix, microcracks, and macrocracks respectively. V_1 is a function of elastic modulus, Poisson's ratio, inner friction angle and material fraction toughness of the matrix. V_2 can be expressed as a function of microcracks parameters such as half length, shape ratio and density of microcracks. Whereas, V_3 for macrocracks is ultrasonic wave velocity in the air (340 m/s). Increase of elastic modulus and material fracture toughness results in the increase of V_1, while the increase of density of microcracks leads to decrease of V_2.

UPV is mostly influenced by V_1 for uncracked samples and it is close to the intact concrete matrix due to less volume of microcracks in the uncracked sample. Once the concrete is cracked, the uncracked matrix volume i_1 decreases greatly, while i_2 and i_3 increase consistently. Cracking of concrete results in the rise of microcracks density that leads to a decrease of V_2, thus UPV of cracked concrete decreases greatly. Once the cracked samples are cured in water for self-healing, re-hydration products of unreacted cement particles crystallized inside the cracks that result in a decrease of i_2 and i_3. The crystallization also changes the inner microcracks and porous structure that results in an increase of V_2, thus UPV of self-healed concrete is expected to increase.

Table 10: UPV results for samples pre-cracked at 28 days

Mix design	Sample name	UPV (Km/s) ± STDV)				
		28 days uncracked (V_0)	28 days pre - cracked (V_p)	21 days healed	Damaged degree, $D = 1-(V_p/V_0)$	Self healing ratio $SR = (V_{21}-V_p)/V_p$
Cxx	C1 Top	5.08 ± 0	1.63 ± 0.01	2.79 ± 0.03	0.68	0.71
	C1 Middle	5.13 ± 0.02	1.51 ± 0	2.66 ± 0.02	0.71	0.77
	C1 Bottom	5.18 ± 0	1.87 ± 0.16	2.91 ± 0.01	0.64	0.55
	C2 Top	5.14 ± 0.04	2.13 ± 0.12	3.67 ± 0.02	0.59	0.72
	C2 Middle	5.08 ± 0.01	2.99 ± 0.11	4.06 ± 0.36	0.41	0.36
	C2 Bottom	5.13 ± 0.03	1.41 ± 0.06	2.85 ± 0	0.72	1.02
	C3 Top	5.15 ± 0	2.16 ± 0.04	2.47 ± 0	0.58	0.14
	C3 Middle	5.13 ± 0.02	1.27 ± 0.07	2.39 ± 0.03	0.75	0.89
	C3 Bottom	5.13 ± 0.03	2.15 ± 0.02	2.85 ± 0	0.58	0.32
0.5Cxx	0.5C1 Top	4.96 ± 0.01	0.61 ± 0.13	4.64 ± 0.01	0.88	6.64
	0.5C1 Middle	4.75 ± 0.01	1.5 ± 0.01	4.59 ± 0.01	0.68	2.06
	0.5C1 Bottom	4.91 ± 0.01	1.19 ± 0.05	4.57 ± 0.01	0.76	2.84
	0.5C2 Top	4.93 ± 0	1.77 ± 0.13	4.94 ± 0.01	0.64	1.79
	0.5C2 Middle	4.84 ± 0.03	1.75 ± 0.08	3.03 ± 0.08	0.64	0.73
	0.5C2 Bottom	4.85 ± 0.02	1.46 ± 0.07	2.5 ± 0.02	0.70	0.72
	0.5C3 Top	4.93 ± 0.01	0.79 ± 0	4.77 ± 0.08	0.84	5.08
	0.5C3 Middle	4.82 ± 0.01	1.42 ± 0	2.73 ± 0.02	0.71	0.93
	0.5C3 Bottom	4.83 ± 0	1.11 ± 0.01	4.41 ± 0.02	0.77	2.96
	0.5C4 Top	4.93 ± 0.01	1.79 ± 0.09	4.83 ± 0	0.64	1.70
	0.5C4 Middle	4.78 ± 0.01	1.99 ± 0.06	4.39 ± 0.25	0.58	1.21
	0.5C4 Bottom	4.83 ± 0.02	1.83 ± 0.02	3.79 ± 0.09	0.62	1.07

From Figure 24, it appears that the presence of fibers decreases the UPV slightly for uncracked samples. This is expected as UPV through cellulose is lower than concrete. Cracking decreases the UPV for both mixes which indicates the discontinuity due to cracking. It can be observed that curing time results in an increase in UPV for both mixes

which indicates the autogenous healing process working well inside the cracks. CeFRC results in 48.7% higher UPV than normal concrete after 21 days of healing that indicates an enhancement of autogenous self-healing due to the addition of fibers.

It can also be observed that controlled and only fiber mortar samples showed a *SR* of 0.62 and 1.46 respectively. This can be attributed due to continued hydration process of unhydrated cement particles and precipitation of calcium carbonate due to carbonation of calcium hydroxide, one of the major hydration products of cement. Fiber concrete results in more *SR* as compared to control concrete indicating that cellulose fibers are effective in improvement of autogenous healing of concrete because they have the tendency to absorb water up to 85% of their weight and act as a water reservoir inside the concrete matrix for improved internal curing.

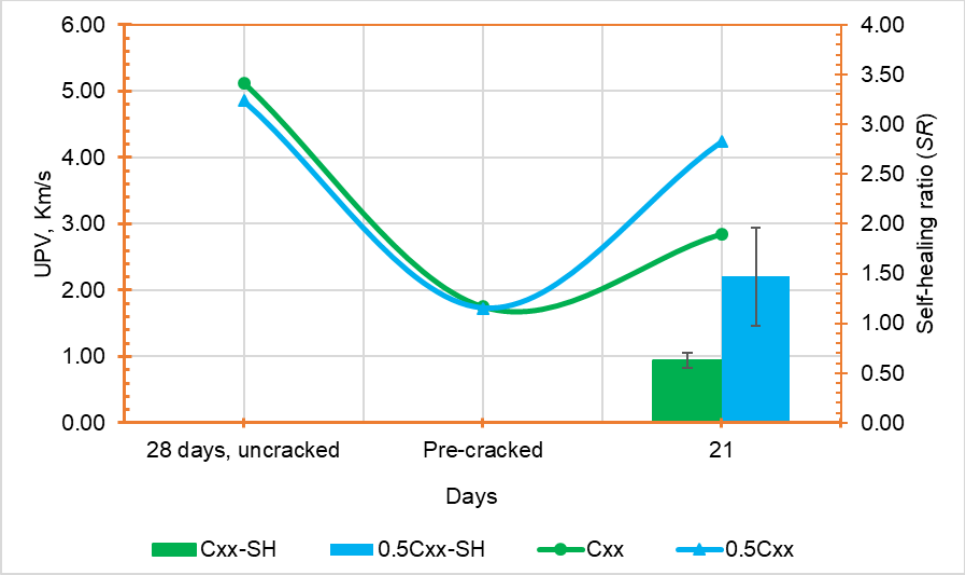

Figure 24: UPV at different days of curing and *SR* for both mixes (*D* = 0.6 to 0.7) cracked at 28 days

Figure 25 represents the relation between damaged degree and self-healing ratio for samples pre-cracked at the age of 28 days. It appears that *SR* is virtually dependent on the damaged degree. It can be observed that *SR* is increased as *D* increases for both mixes. CeFRC shows higher *SR* than normal mix for all damaged degrees indicates the effectiveness of cellulose fiber addition on the autogenous healing of concrete. However, a significantly larger *SR* at higher damaged degree was observed in CeFRC than normal concrete. This is because higher *D* results in more availability of water through microcracks

and availability of cellulose fibers inside the crack improves the bridging of new hydration products across the cracks. However, the new hydration products in normal concrete are not able to bridge the crack at a higher damaged degree that results in lower *SR* as compared to CeFRC. Zhong and Yao also defined a damaged threshold beyond that self-healing decreases as *D* increases, for normal concrete damage threshold is about 0.6-0.7 [58].

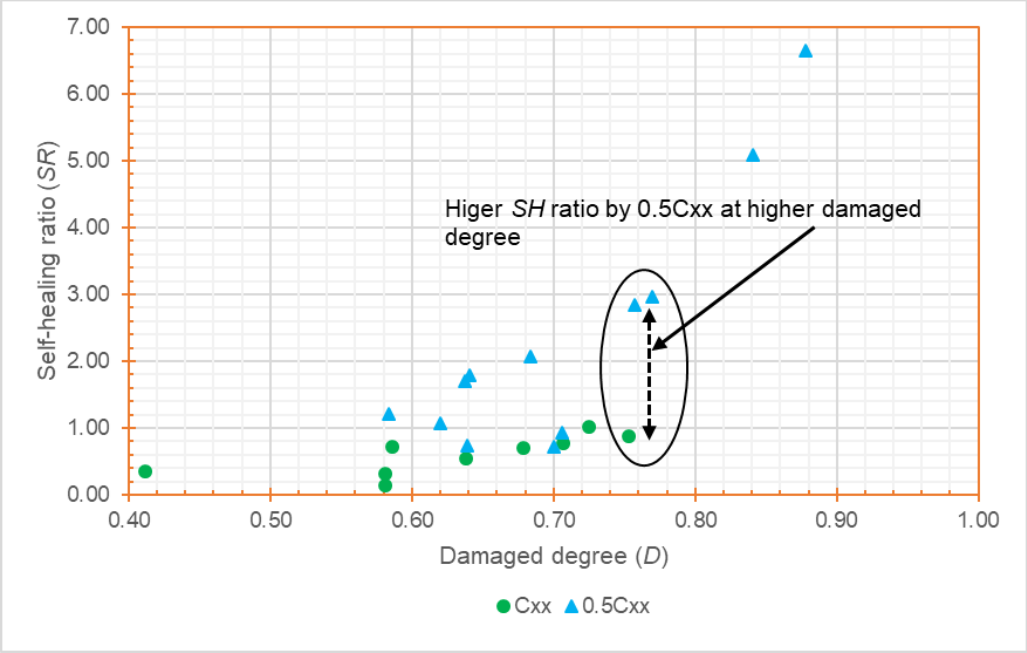

Figure 25: *D* and *SR* relations of samples pre-cracked at 28 days

3.5. Self- Healing Test Results

The surface crack width, theoretical crack width, initial flow rate and healing ratio of three cylinders for both concrete mixes are represented in Table 11. The effect of healing was calculated by introducing a healing ratio (*HR*) parameter as shown below [50, 59]:

$$Healing\ Ratio = 1 - \frac{Final\ flow\ rate}{Initial\ flow\ rate} = 1 - \frac{q_F}{q_0} > 0 \qquad (7)$$

Where q_0 is the initial water flow (lit/min) and q_F is the final water flow measured after a healing period of 28 days. Edvardsen proposed a model to determine the relation between crack width and the water flow passing through the crack [60]. The model is shown in equation (8).

$$q_0 \left(\frac{litres}{hour}\right) = 740 \times I \times CW_{avg}^3 \times K_t \qquad (8)$$

Where q_0 is the initial water leakage per meter visible crack length (lit/h); I is the hydraulic gradient, m of water head/(m); CW_{avg} is the average crack width at the surface (mm); k_t is factor comprising different water temperature (k_t = 1 for water at 20° C with viscosity of 1 mm^2/s). This expression can be modified to the parameters of this study by changing the crack length (considered 75mm, as some part of crack covered with sealant) and other units and can be re-written as shown in equation (9).

$$q_0\left(\frac{litres}{min}\right) = 740 \times \frac{1.7}{0.2} \times CW_{avg}^3 \times 1 \times 0.075 \times \frac{1}{60} = 7.863 CW_{avg}^3 \Rightarrow CW_{avg} = \sqrt[3]{q_0/7.863} \qquad (9)$$

The theoretical surface crack width of all samples was calculated from equation (9) by using the initial flow rate of water. Samples with almost similar actual and theoretical crack width in Table 11 were compared for healing ratio. C6 with actual surface crack width of 0.865 mm and theoretical crack width of 0.48 mm was compared with averaged actual and theoretical crack width for 0.5C6 and 0.5C7, 0.8625 mm and 0.49 mm respectively. It can be observed that CeFRC exhibits a slightly less average healing ratio of 0.609 as compared to 0.628 of normal concrete for crack width of 0.86 mm after 28 days of the healing period.

Table 11: Measured crack width, theoretical crack width, initial flow and the healing ratio of concrete mixes.

Sample ID		Surface crack width (mm)				Theoretical crack width from equation (9) (mm)	Real initial flow q_0 (lit/min)	Healing ratio (*HR*)
		Top	Bottom	Average				
Control	C5	0.7	0.2	0.45	0.578	0.35	0.34	0.765
	C6	0.43	1.3	0.865		0.48	0.86	0.628
	C7	0.33	0.51	0.42		0.36	0.36	0.806
CeFRC	0.5C5	0.43	0.34	0.385	0.703	0.21	0.07	0.857
	0.5C6	1.25	0.54	0.895		0.52	1.11	0.459
	0.5C7	0.73	0.93	0.83		0.46	0.75	0.76

Figure 26 shows the relationship between healing ratio and time for both concrete mixes. It can be observed healing ratio increased with time of healing for both mixtures. However, cellulose fiber concrete exhibits a higher rate of healing in the initial 8 days, followed by a moderately higher healing rate from day 8 to 20 as compared to control concrete. After 20 days, both mixes demonstrate almost similar healing rate.

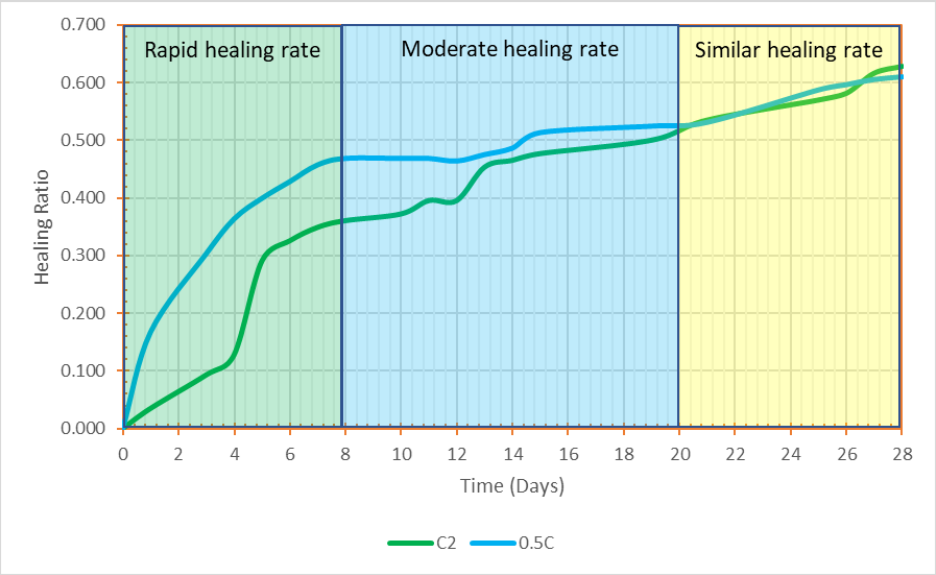

Figure 26: Healing ratio vs Time for both concrete mixes

Author hypothesize that rapid healing rate of CeFRC in the initial healing period can be improved by using other self-healing ingredients in concrete like crystallize admixtures, bacterial and capsule-based ingredients, etc.

In the next chapter, the self-healing properties of bacteria-based mortar are analyzed by using cellulose fibers as a bacteria-carrier.

Chapter 4. Results and Discussion for Self-healing Mortar

In the previous chapter, it was figured out that the addition of cellulose fibers results in the improvement of autogenous healing of concrete. Based on these results the cellulose fibers were used with bacteria-based self-healing mortar as a bacteria carrier to further improve the self-healing efficiency of mortar. In this chapter, the test results for self-healing mortar are presented and discussed.

4.1. Self-Healing Based on Image Analysis

Table 12 shows the crack widths for samples pre-cracked at the age of 14 and 28 days of curing for all mixes.

Table 12: Average crack width of pre-cracked samples

Mix Design	14 days cured		28 days cured	
	Sample Name	Average Crack Width (mm)	Sample Name	Average Crack Width (mm)
CMxx	CM1	0.46	CM6	0.58
	CM2	0.62	CM7	0.61
	CM3	0.54	CM8	0.50
	CM4	0.5	-	-
C0.5Mxx	C0.5M1	0.27	C0.5M6	0.29
	C0.5M2	0.80	C0.5M7	0.27
	C0.5M3	0.31	C0.5M8	0.38
	C0.5M4	0.29	C0.5M9	0.38
	C0.5M5	0.30	C0.5M10	0.37
BL0.5Mxx	BL0.5M1	0.49	BL0.5M6	0.59
	BL0.5M2	0.68	BL0.5M7	0.70
	BL0.5M3	0.69	BL0.5M8	0.67
	BL0.5M4	0.45	BL0.5M9	0.58
B0.5Mxx	B0.5M1	0.56	B0.5M6	0.50
	B0.5M2	0.57	B0.5M7	0.68
	B0.5M3	0.74	B0.5M8	0.63
	B0.5M4	0.60	-	-

Images were analyzed to determine the average crack width of the samples for different stages of self-healing by using *imageJ* software. First, area and length of crack were determined. The average width of the crack was determined using the following formula:

Width of Crack = Area of Crack/Length of Crack

No visible healing of the cracks was observed on the surface of the cracks in image analysis for all type of mixes. Figure 27 (a) shows a set of sample images for B0.5M1 mortar sample pre-cracked at 14 days of curing and observed for crack healing after 7, 14 and 21 days on the front side of the cube. Figure 27 (b) and Figure 27 (c) show the image analysis to measure the crack width of pre-cracked sample on the front and backside of the sample respectively. The average crack width for the sample was calculated from the average of front and backside crack widths.

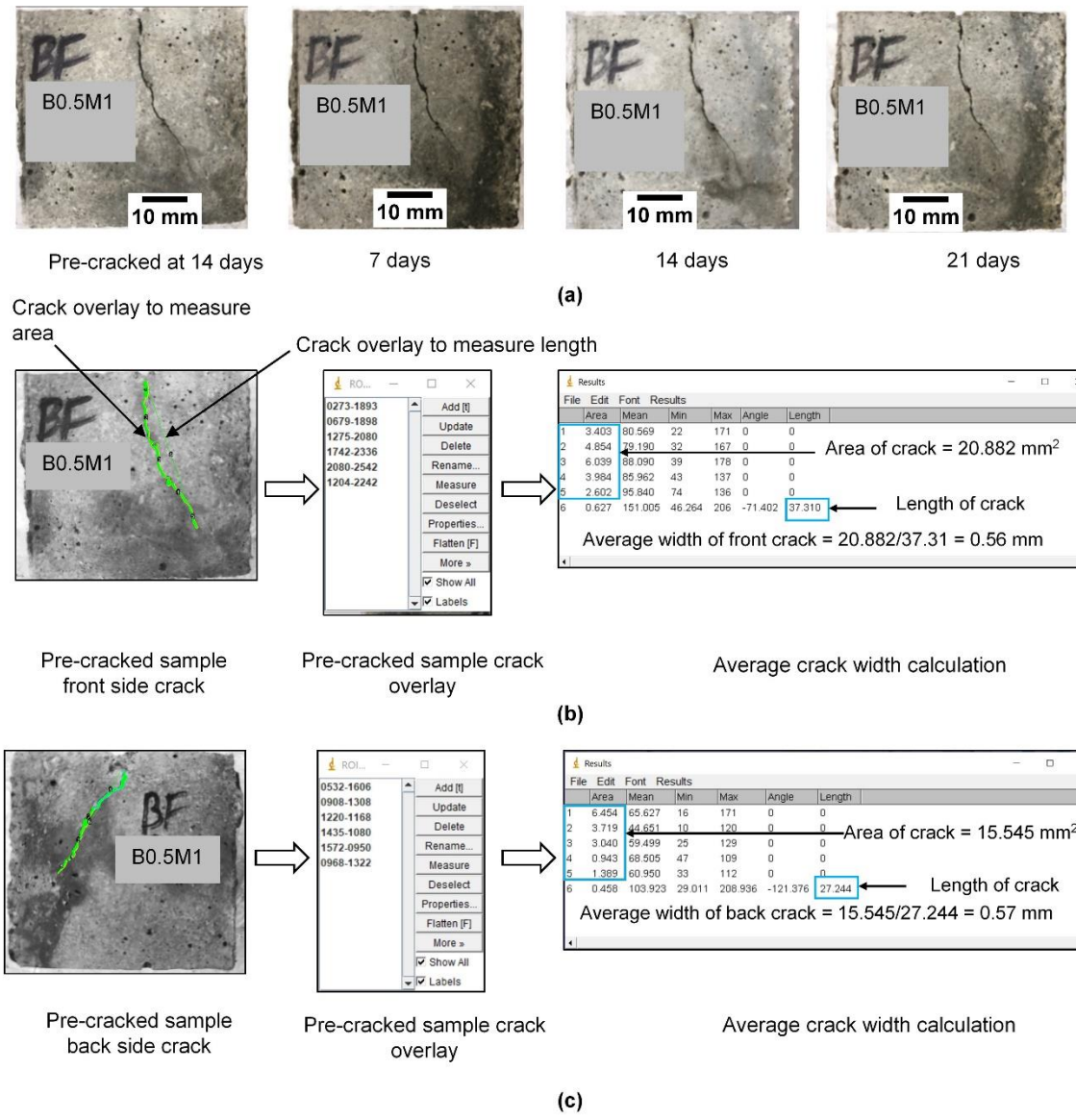

Figure 27. Image analysis for B0.5M1; (a) Image comparison on the front side of the cube; (b) Front side crack; (c) Backside crack.

Crack width = (crack width on front side + crack width on back side)/2 = (0.56+0.57)/2 = 0.56 mm.

4.2. Self-Healing Based on UPV Test

The self-healing performance of all mortar mixes was investigated by the UPV test. The UPV time was recorded for all the mortar samples at different stages of healing across the

crack to study any interior healing of the cracks. For each sample test was repeated at least three times. Data are presented as average ± standard deviation. Table 13 and Table 14 shows the UPV results for all mortars cured for 14 and 28 days respectively.

The damaged degree *D* was calculated using equation (4). A percentage self-healing of mortar, *SH*, that incorporates UPV after 21 days of self-healing and pre-cracked sample can be introduced as:

$$SH = \frac{(V_{21} - V_p)}{V_p} \times 100 \quad (10)$$

Where V_{21} is the UPV after 21 days of self-healing, and V_p is the UPV of pre-cracked sample.

Table 13: UPV results for samples pre-cracked at 14 days

Mix design	Sample name	UPV (km/s) ± STDV					Damaged degree	% Self-healing ± STDV
		14 days uncracked (V_0)	14 days pre-cracked (V_p)	7 days healed	14 days healed	21 days healed (V_{21})	$D = 1-(V_p/V_0)$	$SH = (V_{21}-V_p)$ x100/V_p
CMxx	CM1	4.59 ± 0	3.97 ± 0.07	4.39 ± 0	4.39 ± 0	4.39 ± 0	0.13	10.5 ± 1.9
	CM2	4.46 ± 0.06	4.08 ± 0.06	4.39 ± 0	4.39 ± 0	4.39 ± 0	0.09	7.6 ± 1.7
	CM3	4.53 ± 0.04	4.16 ± 0.03	4.39 ± 0	4.39 ± 0	4.39 ± 0	0.08	5.6 ± 0.8
	CM4	4.53 ± 0.04	4.02 ± 0.02	4.2 ± 0	4.39 ± 0	4.39 ± 0	0.11	9.1 ± 0.4
C0.5Mxx	C0.5M1	4.26 ± 0.09	3.26 ± 0.02	3.46 ± 0.01	3.61 ± 0.01	3.73 ± 0	0.24	14.4 ± 0.7
	C0.5M2	4.4 ± 0.02	3.9 ± 0.01	4 ± 0	4.13 ± 0	4.2 ± 0	0.11	7.8 ± 0.4
	C0.5M3	4.39 ± 0	3.98 ± 0.03	4.11 ± 0.02	4.17 ± 0	4.24 ± 0	0.09	6.5 ± 0.8
	C0.5M4	4.39 ± 0	3.92 ± 0.01	4.09 ± 0.02	4.13 ± 0	4.17 ± 0	0.11	6.4 ± 0.4
	C0.5M5	4.37 ± 0.02	3.82 ± 0	4 ± 0	4.1 ± 0	4.17 ± 0	0.13	9.2 ± 0
BL0.5Mxx	BL0.5M1	4.39 ± 0	3.55 ± 0.02	3.88 ± 0	3.93 ± 0.07	4.03 ± 0	0.19	13.4 ± 0.8
	BL0.5M2	4.2 ± 0	2.12 ± 0.01	4.03 ± 0	4.2 ± 0	4.2 ± 0	0.50	98.3 ± 1.4
	BL0.5M3	4.37 ± 0.05	2.71 ± 0.01	3.73 ± 0	3.98 ± 0.07	4.2 ± 0	0.38	54.9 ± 0.4
	BL0.5M4	4.37 ± 0.08	3.8 ± 0.01	3.88 ± 0	4.2 ± 0	4.2 ± 0	0.13	10.6 ± 0.4
B0.5Mxx	B0.5M1	4.6 ± 0.02	2.3 ± 0.01	3.66 ± 0.06	3.73 ± 0	3.9 ± 0.03	0.50	69.1 ± 1.8
	B0.5M2	4.4 ± 0.02	3.88 ± 0.02	4.2 ± 0	4.2 ± 0	4.24 ± 0	0.12	9.3 ± 0.7
	B0.5M3	4.6 ± 0.02	2.16 ± 0	3.98 ± 0.07	4.1 ± 0	4.2 ± 0	0.53	94.7 ± 0.4
	B0.5M4	4.39 ± 0	2.76 ± 0.01	4.01 ± 0.03	4.05 ± 0.03	4.2 ± 0	0.37	52.1 ± 0.7

Table 14: UPV results for samples pre-cracked at 28 days

Mix design	Sample name	UPV (km/s) ± STDV					Damaged degree	% self-healing ± STDV
		28 days uncracked (V_0)	28 days pre - cracked (V_p)	7 days healed	14 days healed	21 days healed (V_{21})	D = 1-(V_p/V_0)	SH = (V_{21}-V_p) x100/V_p
CMxx	CM6	4.59 ± 0	3.95 ± 0.06	4.2 ± 0	4.2 ± 0	4.2 ± 0	0.14	6.3 ± 1.6
	CM7	4.59 ± 0	4.03 ± 0	4.39 ± 0	4.39 ± 0	4.39 ± 0	0.12	8.8 ± 0
	CM8	4.6 ± 0.04	4.14 ± 0.07	4.39 ± 0	4.39 ± 0	4.39 ± 0	0.10	5.8 ± 1.7
C0.5Mxx	C0.5M6	4.39 ± 0	3.92 ± 0.01	4.23 ± 0.02	4.24 ± 0	4.24 ± 0	0.11	8.2 ± 0.4
	C0.5M7	4.55 ± 0.12	3.9 ± 0.01	4.2 ± 0	4.21 ± 0.02	4.23 ± 0.02	0.14	8.5 ± 0.7
	C0.5M8	4.53 ± 0.11	3.55 ± 0.05	3.94 ± 0	3.96 ± 0.01	3.99 ± 0.03	0.22	12.5 ± 1.3
	C0.5M9	4.39 ± 0	3.73 ± 0.04	4.04 ± 0.02	4.09 ± 0.02	4.11 ± 0.02	0.15	10.1 ± 1.4
	C0.5M10	4.39 ± 0	3.98 ± 0.06	4.2 ± 0	4.2 ± 0	4.23 ± 0.02	0.09	6.2 ± 1.4
BL0.5Mxx	BL0.5M6	4.39 ± 0	3.51 ± 0.03	4.2 ± 0	4.2 ± 0	4.36 ± 0.04	0.20	24.1 ± 2
	BL0.5M7	4.36 ± 0.04	3.86 ± 0.03	4.2 ± 0	4.2 ± 0	4.2 ± 0	0.12	9 ± 0.8
	BL0.5M8	4.32 ± 0.05	3.87 ± 0.01	4.03 ± 0	4.2 ± 0	4.2 ± 0	0.11	8.7 ± 0.4
	BL0.5M9	4.32 ± 0.05	3.59 ± 0.01	4.03 ± 0	4.03 ± 0	4.03 ± 0	0.17	12.4 ± 0.4
B0.5Mxx	B0.5M6	4.43 ± 0.06	4.05 ± 0.03	4.2 ± 0	4.2 ± 0	4.2 ± 0	0.08	3.6 ± 0.8
	B0.5M7	4.45 ± 0.05	3.73 ± 0	4.39 ± 0	4.39 ± 0	4.39 ± 0	0.16	17.5 ± 0
	B0.5M8	4.59 ± 0	3.89 ± 0.01	4.39 ± 0	4.39 ± 0	4.39 ± 0	0.15	12.9 ± 0.4

Mixes were compared based on the damaged degree instead of crack widths because induced cracks have varying widths and depths. Based on the availability and distribution of results, the data were averaged for damaged degree between 0.1 to 0.2 for all mixes. Figure 28 and Figure 29 show the curing days-UPV relation and *SH* for 14 and 28 days aged pre-cracked samples, respectively for *D* between 0.1 to 0.2 for all mixes.

From Figure 28 and Figure 29, it appears that the presence of fibers decreases the UPV slightly for uncracked samples. This is expected as UPV through cellulose is lower than mortar. This trend is observed both at 14 and 28 days. Cracking decreases the UPV for all mixes which indicates the discontinuity due to cracking. It can be observed, curing time results in an increase in UPV for all mixes, indicates the self-healing process working well inside the cracks.

From Figure 28, it can be observed, controlled and only fiber mortar samples showed a *SH* of 9.8% and 7.8% respectively. This can be attributed due to continued hydration process of unhydrated cement particles at an early age. 9.32% self-healing is observed in the B0.5Mxx, more than mortar containing only fibers. Mix BL0.5Mxx incorporated with

cellulose fiber as a carrier for bacteria, and nutrients are provided inside the mix shows 12.04% *SH*, maximum as compared to other mixes. This is due to the availability of calcium lactate throughout the matrix for the MICP, which results in the additional production of calcium carbonate due to the carbonation of calcium hydroxide, one of the major hydration products of cement. However, in case of B0.5Mxx calcium lactate is only present in cracked region through curing water causes MICP and carbonation of calcium hydroxide possible only in the cracked region instead of the whole matrix like BL0.5Mxx, results in slightly less *SH* as compared to BL0.5Mxx for samples cracked at an early age.

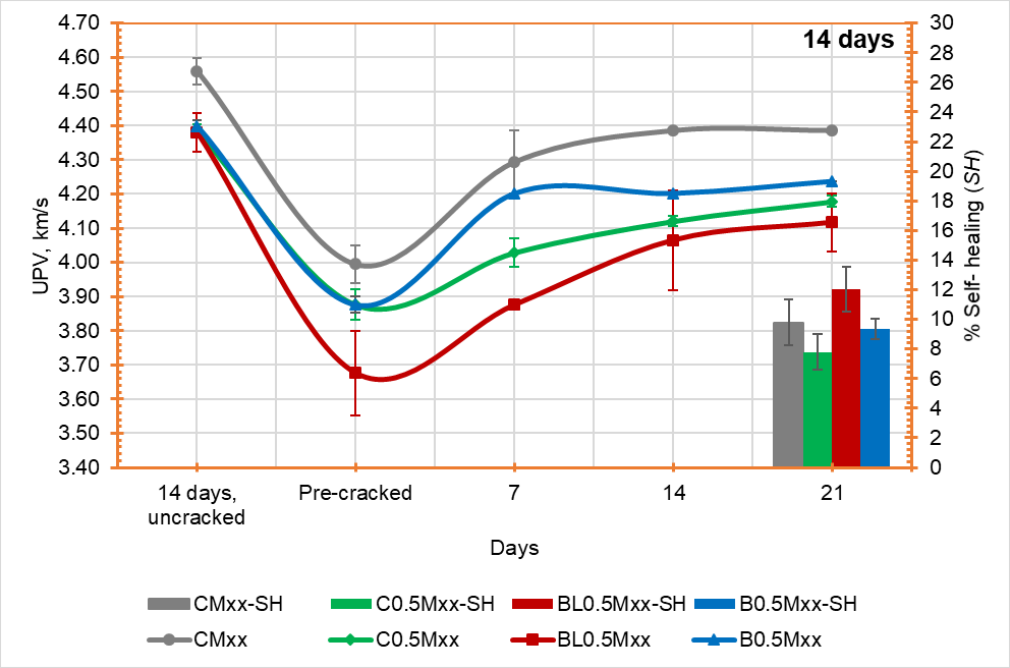

Figure 28. UPV at different days of curing and *SH* for all mixes (D = 0.1 to 0.2) pre-cracked at 14 days

Figure 29 illustrates the self-healing for samples pre-cracked at 28 days of curing. It can be observed *SH* in control mortar is decreased to 6.97% for 28 days pre-cracked samples as compared to 9.8% for 14 days pre-cracked samples. This exhibit, there are less unhydrated cement grains to contribute for the self-healing at later age. Both bacterial mixes, BL0.5Mxx and B0.5Mxx show the higher *SH* than control and only fiber mix, 10%, and 15.2% respectively. Like control mix, BL0.5Mxx results in a decrease in *SH* for samples pre-cracked at 28 days as compared to 14 days. Because at 28 days age there is less availability of calcium hydroxide to produce calcium carbonate inside the matrix and

lower availability of calcium lactate in the cracked region for MICP. However, in the case of B0.5Mxx more calcium lactate from curing water is present in the cracked region for MICP results in maximum self-healing performance among all mixes.

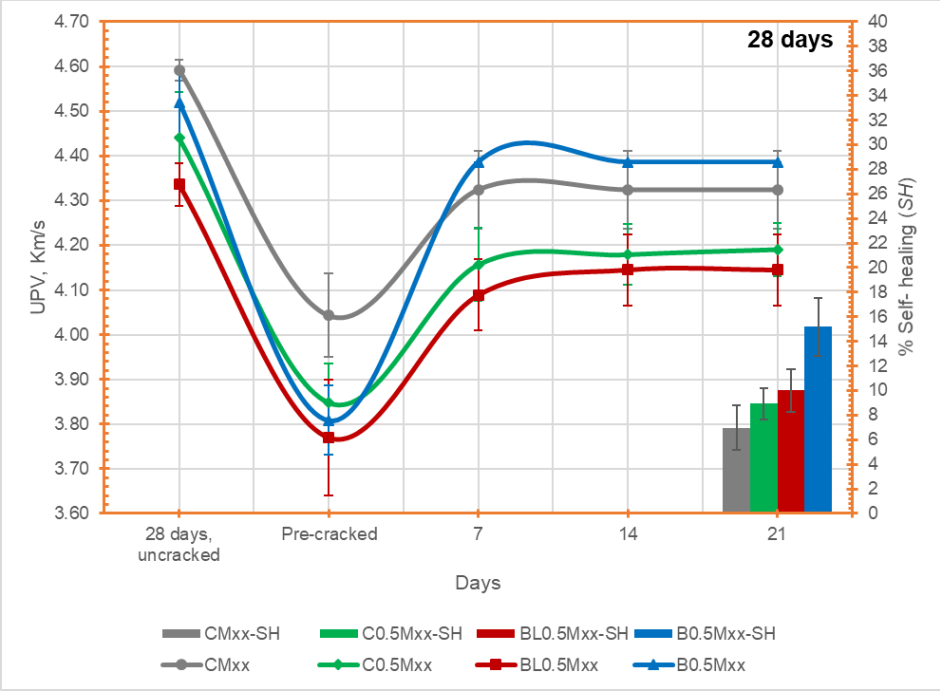

Figure 29. UPV at different days of curing and *SH* for all mixes (D = 0.1 to 0.2) pre-cracked at 28 days

Figure 30 and Figure 31 represents the relation between damaged degree and percentage self-healing for samples pre-cracked at the age of 14 and 28 days respectively. It appears that *SH* is virtually dependent on the damaged degree when the results are presented as trendlines. It can be observed that *SH* is increased as *D* increases for all mixes pre-cracked at 14 and 28 days. Bacterial mixes show significant improvement in *SH* at higher damaged degree, BL0.5Mxx results in 13.2% and 64.1% more *SH* than control mix at *D* of 0.2 and 0.5 respectively, for 14 days pre-cracked samples (see Figure 30). Similarly, 3.18% and 11.62% more *SH* are observed in B0.5Mxx at D of 0.12 and 0.2 respectively, for samples pre-cracked at 28 days (see Figure 31). This is because, higher *D* results in more availability of water and oxygen through microcracks, which improves the MICP, leads to a higher value of *SH* at increased *D*. However, Zhong and Yao defined a damaged threshold beyond

that self-healing decreases as *D* increases, for normal concrete damage threshold is about 0.6-0.7 [58].

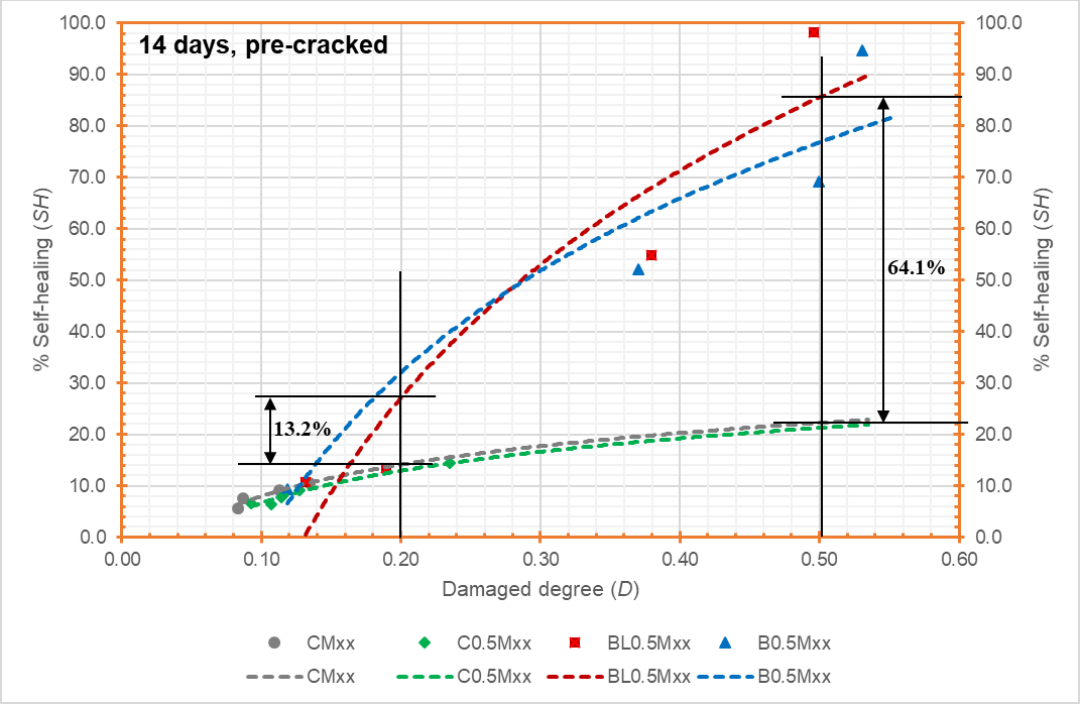

Figure 30. *D* and *SH* relations of samples pre-cracked at 14 days

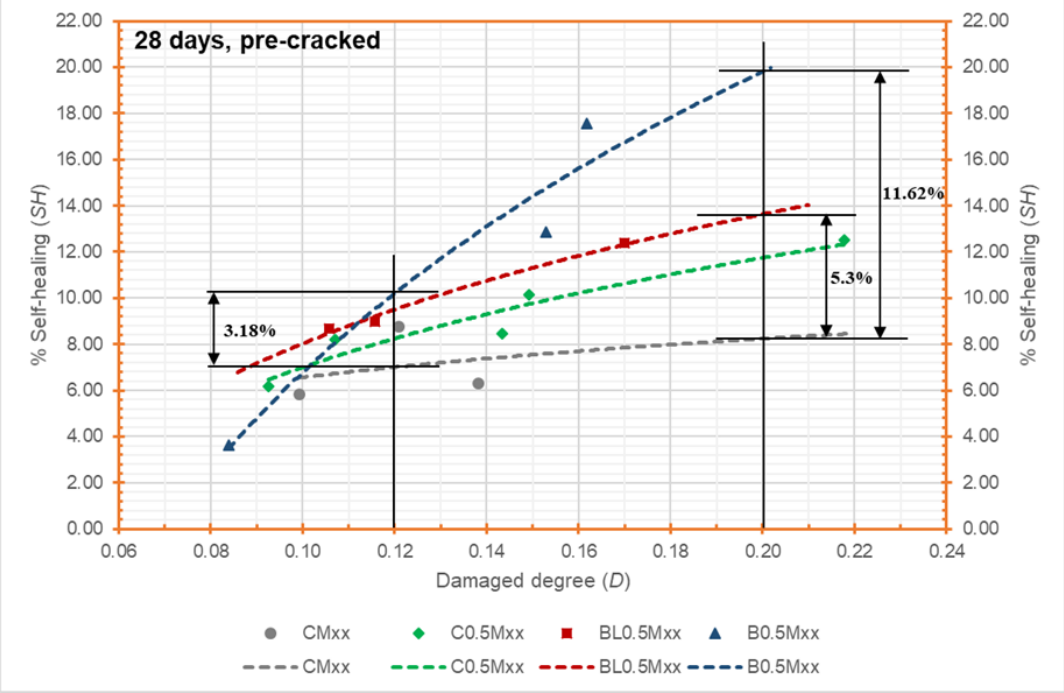

Figure 31. *D* and *SH* relations of samples pre-cracked at 28 days

Relating, Figure 30 and Figure 31, demonstrate a decrease in *SH* of bacterial mixes with age of pre-cracking, 13.2% to 5.3% decrease in *SH* for BL0.5Mxx for D of 0.2. This decrease in *SH* of bacterial mixes can be due to continued hydration reaction in mortar resulting in the development of dense microstructure at later age. The dense matrix creates pressure on the fibers and free bacteria, leads to a decrease in the viability of bacteria and therefore, the self-healing process decreased at later age. Additionally, at a later age, less availability of calcium hydroxide from cement hydration reaction leads to lower precipitation of calcium carbonate from the carbonation of calcium hydroxide.

Even after a decrease in *SH* with age, both mixes with bacteria encapsulated in fibers exhibit higher *SH* than control and only fiber mixes. Therefore, the technique using cellulose fiber as a bacteria-carrier was effective and improved the self-healing capacity of control mortar.

4.3. Compressive Strength

28 days compressive strength for all four mixes was measured as per ASTM C579 [56] after wet curing. Table 15 shows the compressive strength of each mix along with averages and standard deviation values. The data in Table 15 were analyzed for the % change in compressive strength from control mortar for all mixes. The % change in compressive strength for 28 days cured mortar is shown in Figure 32.

A decrease in compressive strength of mortar by 6.97% is noticed with addition of 0.5% fibers. The decrease in compressive strength is significantly less than the concrete results in chapter 3 after addition of 0.5% fibers and this can be understood from the quantities of cement used in the mix design of concrete and mortar. The mortar had a cement content of 736 Kg available per cubic meter as compared to only 340 Kg/m^3 in concrete, this could lead to an overall increase in hydration reaction in mortar as compared to concrete.

Out of two bacterial mortar mixes, the maximum decrease in compressive strength is for BL0.5Mxx mix, 33.11%. However, a decrease of 22.09% in compressive strength is observed for the B0.5Mxx mix. Overall, it can be observed that the addition of bacteria and fibers results in a decrease in compressive strength of mortar. The more decrease in compressive strength is noticed in the mix containing calcium lactate. This is due to

calcium lactate added to mortar do not take part in hydration of cement directly, instead, the by-product, calcium carbonate produced inside the mortar matrix and excess production of calcium carbonate inside the matrix causes reduction of compressive strength [61]. Opposite to this, mortar sample containing fiber and bacteria, cured in calcium lactate (B0.5Mxx) results in a lower decrease in compressive strength. However, the loss in strength is only for the limited mixes with 0.5% of fiber concentration and 1.3 x 10^7 bacteria/cm^3 concentration of bacteria.

Table 15: Compressive strength test results for cement mortar

Mix Design	**28 days Compressive Strength (MPa)**	
	Individual	**Average ± STDV**
CMxx	48.12	46.58 ± 3.21
	40.4	
	49.54	
	46.82	
	48.04	
C0.5Mxx	42.8	43.34 ± 1.02
	44.82	
	41.8	
	43.32	
	43.94	
BL0.5Mxx	30.5	31.16 ± 1.74
	32.3	
	28.54	
	30.78	
	33.68	
B0.5Mxx	39.36	36.29 ± 1.92
	34.04	
	35.88	
	35.9	

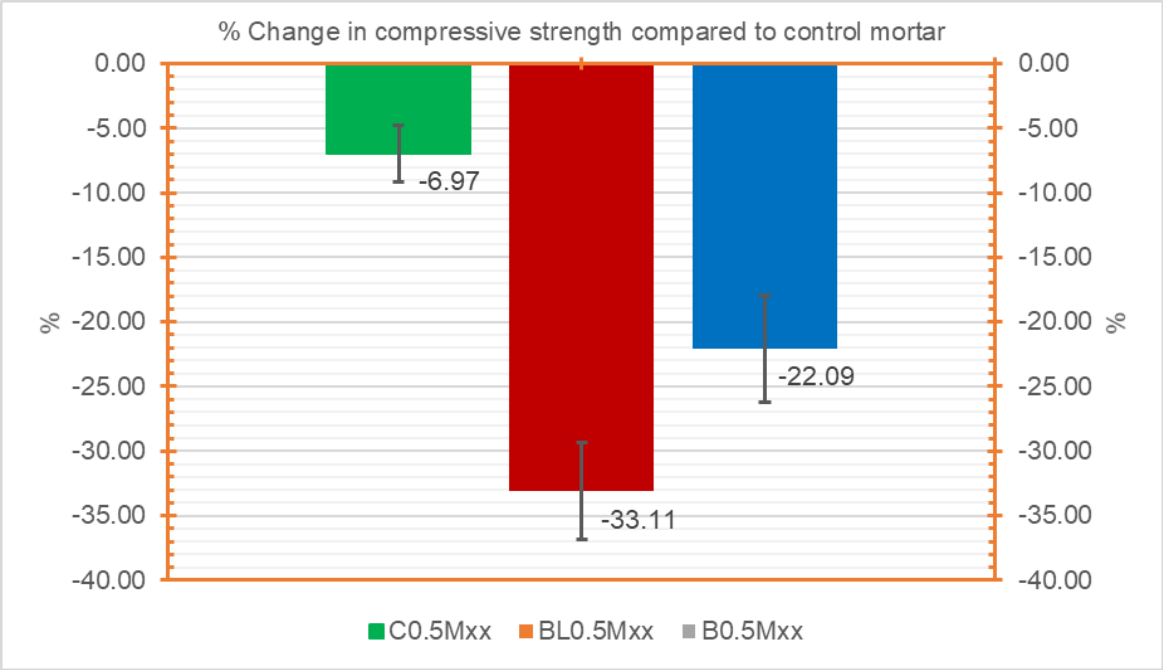

Figure 32. % Change in compressive strength compared to control mortar

The change in compressive strength with different concentration of fibers, nutrients, and bacteria needs further investigation. The B0.5Mxx mix cured in water containing calcium lactate performed well to maintain the strength of mortar out of both bacterial mixes. So, it is observed that providing bacterial nutrients from outside during curing instead of inside while mixing helps to maintain the mortar strength properties.

4.4. Cost analysis of various bacteria-carriers

The cost for different bacteria-carriers is determined and compared for a cubic meter of concrete. The concrete mix design with a strength of 32 MPa is considered for the material calculation. The quantity considered for cement, aggregates, sand, and water is 340, 1120, 820 and 181 kg/m^3 respectively. Estimated costs for various bacteria-carriers is represented in Table 16. Figure 33 shows the prices in US dollars for different carrier materials required for a cubic meter of concrete at dosages stated in Table 16.

Table 16: Costs for various bacteria-carriers per cubic meter of concrete

Bacteria-carrier	Quantity	Unit Price (USD)	USD/m³ of concrete	Remarks
Epoxy	20.4 kg/m³ (6% weight of cement [19])	47.6 per 3.78 Liter [62]	205	Density =1250 kg/m³
Ceramsite	266.56 kg/m³ (78.4% weight of cement [18])	0.3 per kg [63]	80	-
Expanded clay particles	258.54 kg/m³ (76.04% weight of cement [17])	150 per m³ [64]	111	Density =350 kg/m³ [64]
Expanded perlite	80.24 kg/m³ (23.6% weight of cement [65])	1.5 per kg [66]	120	-
Hydrogel	17 kg/m³ (5% weight of cement [20])	3.5 per kg [67]	60	-
Melamine	17 kg/m³ (5% weight of cement [21])	1.2 per kg [68]	20	-
Cellulose fiber	5.5 kg/m³ (0.5% of volume)	2.46 per kg [14]	14	Density =1100 kg/m³

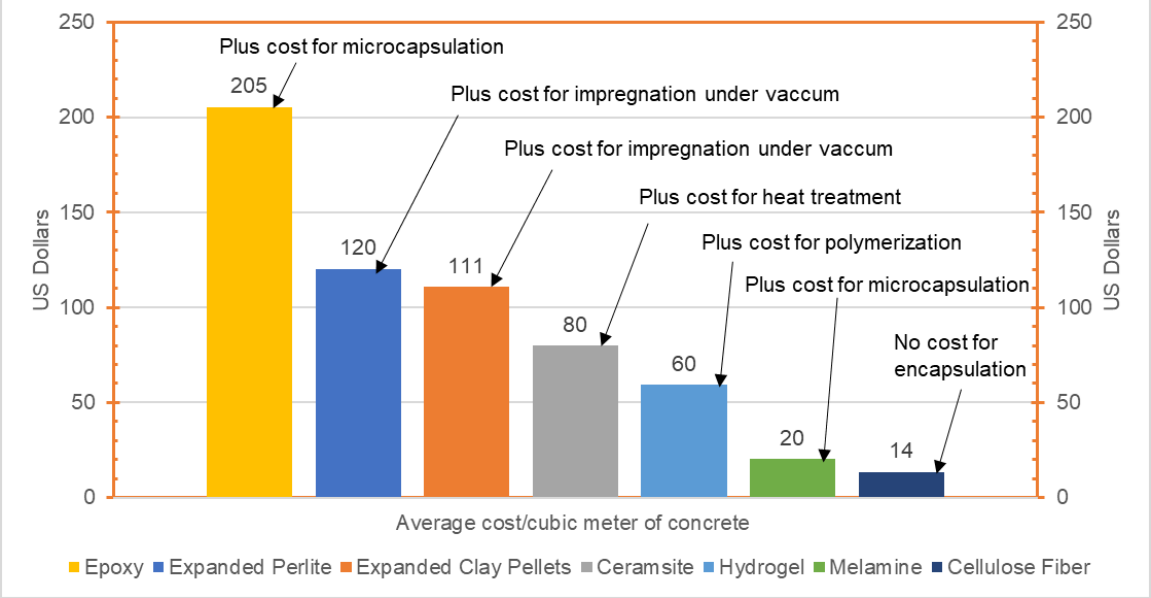

Figure 33. Material Cost in US dollars for different bacteria-carriers per m³ of concrete

Cellulose fibers have the lowest material cost as compared to other bacteria-carriers. Additionally, the cost for encapsulating bacteria is zero.

After comparing different carrier materials based on the encapsulation technique and cost analysis, it is obvious that the method of use cellulose fibers as a carrier for bacteria is a promising option. Moreover, cellulose fiber improves the crack resistance of concrete and they are suitable to use in a ready mix plant. Also, due to the high absorption rate, fibers can act as water reservoirs for promoting internal curing. Therefore, the method of using cellulose fiber as bacteria-carrier for self-healing concrete has the potential to be more widely used for large scale concrete structures.

Chapter 5. Conclusions and Future Work

5.1. Conclusions Based on the Concrete Study

- 0.5% volume fraction of cellulose fibers results in a decrease in compressive strength of control concrete due to replacement of part of concrete matrix with cellulose fibers that leads to lower workability and compaction of concrete.
- Cellulose fiber results in an increase in flexural strength of normal concrete by 7.84% and a considerable increase in maximum deflection are also observed. This indicates good fiber bond and their suitability for use as a reinforcement in concrete.
- Concrete with cellulose fibers had a 24% lower water penetration depth and 42% lower coefficient of permeability compared to control concrete, indicated the improvement in water tightness of concrete. Average water penetration depths seemed to be a better option to calculate the coefficient of permeability as compared to maximum penetration depths.
- Cellulose fiber acts as a water reservoir and results in better internal curing of concrete. A higher self-healing ratio and 48.7% higher UPV velocity were observed in CeFRC as compared to normal concrete after 21 days of self-healing with damaged degree between 0.6 to 0.7, indicates improvement of autogenous healing of concrete due to the addition of cellulose fiber.
- Self-healing ratio of CeFRC increases significantly than normal concrete at higher damaged degree because fibers inside the crack improve the bridging of new hydration products across the cracks at higher damaged degree, which is not possible in normal concrete.
- CeFRC has a rapid healing rate in the initial days as compared to normal concrete and this property can be enhanced by using with other self-healing concrete ingredients like crystalline admixtures, bacteria and capsule-based ingredients, etc. to improve the self-healing efficiency of concrete.

5.2. Conclusions Based on the Self-healing Mortar Study

- Mortars containing bacteria encapsulated in cellulose fibers result in an increase in UPV with healing time for pre-cracked samples. The increase in UPV indicates the self-healing process is working well inside the crack even with a surface crack that visually does not look filled from the results of image analysis.
- Self-healing mortar performs well when nutrients provided inside the mix for early age pre-cracked samples. However, when samples are pre-cracked at later age, better self-healing is demonstrated by samples with nutrients provided in curing water.
- Using cellulose fiber as a bacteria-carrier (BL0.5Mxx) result in 12.04% self-healing for damaged degree between 0.1 to 0.2, when pre-cracked at 14 days of curing. However, when pre-cracked at 28 days 15.2% (B0.5Mxx) self-healing is observed, 8.23% more than control mortar for damaged degree between 0.1 to 0.2.
- Self-healing efficiency of mortar using cellulose fiber as bacteria-carrier increases significantly with an increase in damaged degree. Mortar with bacteria encapsulated in fiber and nutrients provided inside the mix, resulting in 64.1% more self-healing than control mix for the damaged degree of 0.5, for samples pre-cracked at age of 14 days. Similarly, mortar with bacteria encapsulated in fibers and nutrients provided in curing water, results in 11.62% more self-healing than control mix at the damaged degree of 0.2, for samples pre-cracked at 28 days.
- A decrease in compressive strength is observed for all mixes containing cellulose fiber for the fiber fraction, bacteria and nutrients concentration used in this study. The mixes with different concentrations of fiber, bacteria, and nutrients are needed to be investigated for the change in compressive strength.
- The characteristics like minimum cost as compared to other bacteria-carriers, having easy availability in the cracked region, the simplest method to encapsulate bacteria and suitability for ready mix plant make cellulose fibers a promising bacteria-carrier material for small to large scale concrete construction.

5.3. Future Scope of Work

This work can be further extended to include the following aspects:

- The different volume fraction of cellulose fibers can be used to analyze their impact on the compressive strength of concrete.
- Cellulose fiber can also be used in conjunction with other macro fibers to see the overall improvement in autogenous healing and mechanical properties of concrete.
- Crystalline admixture based self-healing materials can be added to CeFRC to improve the self-healing of concrete.
- Resonant frequency test can be used to determine the self-healing of concrete.
- A higher dosage of cellulose fiber can be used to increase the number of encapsulated bacteria.
- The cellulose fibers can be coated with cement or other coating materials like sodium alginate, geopolymer, etc. to protect the bacteria from leaving the cellulose fiber after encapsulation during mixing in self-healing mortar.
- Cellulose fiber as a bacteria-carrier can be used with other bacteria-carriers to see the combined performance of different bacteria-carriers in self-healing mortar.
- Different concentration of nutrients and bacteria can be investigated for the performance of self-healing mortar.
- In addition to the UPV test, self-healing ratio can be calculated by using the compressive strength of pre-cracked and self-healed samples.

References

[1] H. M. Jonkers, A. Thijssen, G. Muyzer, O. Copuroglu and E. Schlangen, "Application of bacteria as self-healing agent for the development of sustainable concrete," *Ecological Engineering,* vol. 36, no. 2, pp. 230-235, 2010.

[2] S. Luhar and S. Gourav, "A Review Paper on Self Healing Concrete," *Journal of Civil Engineering Research,* vol. 2015, no. 3, pp. 53-58, 2015.

[3] E. Cailleux and V. Pollet, "Investigations on the development of self-healing properties in protective coatings for concrete and repair mortars".

[4] M. Yunovich and N. Thompson, "Corrosion of Highway Bridges: Economic Impact and Control Methodologies," *Concrete International,* vol. 25, no. 1, pp. 52-57, 2003.

[5] H. Haoliang and G. Ye, "A review on self-healing in reinforced concrete structures in view of serving conditions," *In 3rd International Conference on Service Life Design for Infrastructure, Zhuhai, China,* pp. 1-14, 2014.

[6] H. Huang, G. Ye, C. Qian and E. Schlangen, "Self-healing in cementitious materials: Materials, methods and service conditions," *Materials and Design,* vol. 92, pp. 499-511, 15 2 2016.

[7] J. Dick, W. De Windt, B. De Graef, H. Saveyn, P. Van Der Meeren, N. De Belie and W. Verstraete, "Bio-deposition of a calcium carbonate layer on degraded limestone by Bacillus species," *Biodegradation,* vol. 17, no. 4, pp. 357-367, 8 2006.

[8] E. Technology, "Self-healing concrete," *Engineer,* vol. MAY, no. 46, pp. 39-43, 2011.

[9] A. El-Newihy, P. Azarsa, R. Gupta and A. Biparva, "Effect of Polypropylene Fibers on Self-Healing and Dynamic Modulus of Elasticity Recovery of Fiber Reinforced Concrete," *Fibers,* vol. 6, no. 1, p. 9, 1 2 2018.

[10] Victor C. Li, En-Hua Yang, "Self Healing in Concrete Materials," *Self-Healing Materials,* pp. 161-193, 2007.

[11] Y. Yang, M. D. Lepech, E. H. Yang and V. C. Li, "Autogenous healing of engineered cementitious composites under wet-dry cycles," *Cement and Concrete Research,* vol. 39, no. 5, pp. 382-390, 2009.

[12] J. P. Ferreira and F. A. Branco, "The use of glass fiber-reinforced concrete as a structural material," *Experimental Techniques,* vol. 31, no. 3, pp. 64-73, 5 2007.

[13] H. Singh, R. Gupta, "Strength recovery and crack healing of self-healing cement mortar containing cellulose fibers and bacteria," in *1st International Conference on New Horizons in Green Civil Engineering*, Victoria, 2018.

[14] "Cellulose fiber," [Online]. Available: https://www.alibaba.com/product-detail/Cellulose-fiber_1529438436.html?spm=a2700.7724838.2017115.23.24c76d86iHHDcv. [Accessed 09 July 2019].

[15] H. Tian, Y. X. Zhang, C. Yang and Y. Ding, "Recent advances in experimental studies of the mechanical behaviour of natural fibre-reinforced cementitious composites," *Structural Concrete*, vol. 17, no. 4, pp. 564-575, 1 12 2016.

[16] J. Zhang, Y. Liu, T. Feng, M. Zhou, L. Zhao, A. Zhou and Z. Li, "Immobilizing bacteria in expanded perlite for the crack self-healing in concrete," *Construction and Building Materials*, vol. 148, pp. 610-617, 2017.

[17] V. Wiktor and H. M. Jonkers, "Quantification of crack-healing in novel bacteria-based self-healing concrete," *Cement and Concrete Composites*, vol. 33, no. 7, pp. 763-770, 8 2011.

[18] J. Xu, X. Wang, J. Zuo and X. Liu, "Self-Healing of Concrete Cracks by Ceramsite-Loaded Microorganisms," *Advances in Materials Science and Engineering*, vol. 2018, 2018.

[19] B. Dong, G. Fang, W. Ding, Y. Liu, J. Zhang, N. Han and F. Xing, "Self-healing features in cementitious material with urea-formaldehyde/epoxy microcapsules," *Construction and Building Materials*, vol. 106, pp. 608-617, 2016.

[20] J. Y. Wang, D. Snoeck, S. Van Vlierberghe, W. Verstraete and N. De Belie, "Application of hydrogel encapsulated carbonate precipitating bacteria for approaching a realistic self-healing in concrete," *Construction and Building Materials*, vol. 68, pp. 110-119, 2014.

[21] J. Y. Wang, H. Soens, W. Verstraete and N. De Belie, "Self-healing concrete by use of microencapsulated bacterial spores," *Cement and Concrete Research*, vol. 56, pp. 139-152, 2014.

[22] J. Wang, K. Van Tittelboom, N. De Belie and W. Verstraete, "Use of silica gel or polyurethane immobilized bacteria for self-healing concrete," *Construction and Building Materials*, vol. 26, no. 1, pp. 532-540, 2012.

[23] K. Van Tittelboom and N. De Belie, Self-healing in cementitious materials-a review, vol. 6, 2013, pp. 2182-2217.

[24] L. Souza and A. Al-Tabbaa, "Microfluidic fabrication of microcapsules tailored for self-healing in cementitious materials," *Construction and Building Materials,* vol. 184, pp. 713-722, 2018.

[25] W. Khaliq and M. B. Ehsan, "Crack healing in concrete using various bio influenced self-healing techniques," *Construction and Building Materials,* vol. 102, pp. 349-357, 2016.

[26] J. Y. Wang, N. De Belie and W. Verstraete, "Diatomaceous earth as a protective vehicle for bacteria applied for self-healing concrete," *Journal of Industrial Microbiology and Biotechnology,* vol. 39, no. 4, pp. 567-577, 4 2012.

[27] R. Gupta and N. Banthia, "Correlating plastic shrinkage cracking potential of fiber reinforced cement composites with its early-age constitutive response in tension," *Materials and Structures/Materiaux et Constructions,* vol. 49, no. 4, pp. 1499-1509, 2016.

[28] "UltraFiber Technical Bulletin UFTB #1 Plastic Shrinkage Crack Reduction," Google, [Online]. Available: https://drive.google.com/file/d/0ByWupltkC24Lc2hvWTNMVWVoc3M/view. [Accessed 14 June 2019].

[29] "5 Reasons to use Solomon UltraFiber 500," Google, [Online]. Available: https://drive.google.com/file/d/0ByWupltkC24LeUR2MWU1c2ZvOFk/view. [Accessed 14 June 2019].

[30] "UltraFiber Technical Bulletin UFTB #4 Hydration Benefit," Google, [Online]. Available: https://drive.google.com/file/d/0ByWupltkC24LekF5T2drZF9feEE/view. [Accessed 14 June 2019].

[31] "UltraFiber Technical Bulletin UFTB #3 Alkali Resistance," Google, [Online]. Available: https://drive.google.com/file/d/0ByWupltkC24LY09VZkJNcm1icGs/view. [Accessed 14 June 2019].

[32] "UltraFiber Technical Bulletin UFTB #7 Freeze/Thaw Durability," Google, [Online]. Available: https://drive.google.com/file/d/0ByWupltkC24LRkltZlV2OXQzZGs/view. [Accessed 14 June 2019].

[33] "UltraFiber Technical Bulletin UFTB #2 Finishability," Google, [Online]. Available: https://drive.google.com/file/d/0ByWupltkC24LS1VYRTV1ZmstR3c/view. [Accessed 14 June 2019].

[34] ASTM C150/C150M-19a, "Standard specification for Portland cement," *ASTM international.*

[35] "Solomon UltraFiber," [Online]. Available: http://www.ultrafiber500.com/#500. [Accessed 17 June 2019].

[36] P. Soroushian, Shahram Ravanbakhsh, "Control of plastic shrinkage cracking with specialty cellulose fibers," *ACI MATERIALS JOURNAL,* vol. 95, no. 4, pp. 429 - 435, 07 1998.

[37] "500 Product Information," [Online]. Available: https://www.solomoncolors.com/documents/ultrafiber/Technical%20Fiber%20Binder%20-%20500%20Specification.pdf. [Accessed 14 June 2019].

[38] T. Rahmani, B. Kiani, F. Sami, B. N. Fard, Y. Farnam and M. Shekarchizadeh, "Durability of Glass, Polypropylene and Steel Fiber Reinforced Concrete," *International conference on durability of building materials and components,* pp. 1-8, 2011.

[39] "Properties of Polypropylene Fibres | Syntech Fibres," Syntechfibres.com, [Online]. Available: http://syntechfibres.com/polypropylene/properties-of-polypropylen-fibres/. [Accessed 19 September 2019].

[40] B. Dileep, K. Reddy, S. Salma, P. Venkata, S. Krishna and C. K. Mounika, "Experimental Study on Bacterial Concrete," 2017.

[41] "Calcium lactate, CAS No. 814-80-2," i Chemical, [Online]. Available: http://www.ichemical.com/products/814-80-2.html. [Accessed 28 June 2019].

[42] N. Banthia, F. Majdzadeh and J. Wu, "Fiber Synergy in Hybrid Fiber Reinforced Concrete (HyFRC) in Flexure, Shear and Impact," *BEFIB2012 – Fibre reinforced concrete Joaquim Barros et al. (Eds),* vol. 48, pp. 91-97, 2012.

[43] ASTM C192/C192M-15, "Standard Practice for Making and Curing Concrete Test," *ASTM International,* 2015.

[44] C143/C143M − 15a, "Standard Test Method for Slump of Hydraulic-Cement Concrete," *ASTM International,* 2015.

[45] R. Gupta and A. Biparva, "Innovative Test Technique to Evaluate “Self-Sealing” of Concrete," *Journal of Testing and Evaluation,* vol. 43, no. 5, p. 20130285, 14 10 2014.

[46] ASTM C39/C39M-15a, "Standard Test Method for Compressive Strength of Cylindrical Concrete Specimens," *ASTM International,* 2015.

[47] C293/C293M − 16, "Standard Test Method for Flexural Strength of Concrete (Using Simple Beam With Center-Point Loading)," *ASTM International,* 2016.

[48] DIN 1048, "Testing concrete: Testing of hardened concrete (specimens prepared in mould), Deutscher Ausschuß für Stahlbeton of the Normenausschuß Bauwesen," 1991.

[49] M. Ibrahim and M. Issa, "Evaluation of chloride and water penetration in concrete with cement containing limestone and IPA," *Construction and Building Materials,* vol. 129, pp. 278-288, 2016.

[50] P. Azarsa, R. Gupta and A. Biparva, "Assessment of self-healing and durability parameters of concretes incorporating crystalline admixtures and Portland Limestone Cement," *Cement and Concrete Composites,* vol. 99, no. August 2018, pp. 17-31, 2019.

[51] S. F. Selleck, E. N. Landis, M. L. Peterson, S. P. Shah and J. D. Achenbach, "Ultrasonic investigation of concrete with distributed damage," *ACI Materials Journal,* vol. 95, no. 1, pp. 27-36, 1998.

[52] N. F. Ariffin, M. W. Hussin, A. R. Mohd Sam, H. Seung Lee, N. H. Nur, N. H. Abdul Shukor Lim and M. Samadi, "Mechanical properties and self-healing mechanism of epoxy mortar," *Jurnal Teknologi,* vol. 77, no. 12, pp. 37-44, 2015.

[53] M. A. K. Bahrin, M. F. Othman, N. H. N. Azi and M. F. Talib, "Jurnal Teknologi," *Jurnal Teknologi (Sciences & Engineering),* vol. 78, no. 6-13, pp. 137 - 143, 2016.

[54] M. Sarkar, T. Chowdhury, B. Chattopadhyay, R. Gachhui and S. Mandal, "Autonomous bioremediation of a microbial protein (bioremediase) in Pozzolana cementitious composite," *Journal of Materials Science,* vol. 49, no. 13, pp. 4461-4468, 2014.

[55] ASTM C597-16, "Standard Test Method for Pulse Velocity Through Concrete," *ASTM international.*

[56] ASTM C579-18, "Standard test method for compressive strength of chemical-resistant mortars, grouts, monolithic surfacings, and polymer Concretes”.," *ASTM international.*

[57] S. E. Hedegaard and T. C. Hansen, "Water permeability of fly ash concretes," *Materials and Structures,* vol. 25, no. 7, pp. 381-387, 1992.

[58] W. Zhong and W. Yao, "Influence of damage degree on self-healing of concrete," *Construction and Building Materials,* vol. 22, no. 6, pp. 1137-1142, 2008.

[59] M. Roig-Flores, F. Pirritano, P. Serna and L. Ferrara, "Effect of crystalline admixtures on the self-healing capability of early-age concrete studied by means of permeability and crack closing tests," *Construction and Building Materials,* vol. 114, pp. 447-457, 2016.

[60] C. Edvardsen, "Water permeability and autogenous healing of cracks in concrete," *ACI Materials Journal,* vol. 96, no. 4, pp. 448-454, 1999.

[61] K. Vijay and M. Murmu, "Effect of calcium lactate on compressive strength and self-healing of cracks in microbial concrete," *Frontiers of Structural and Civil Engineering,* vol. 13, no. 3, pp. 515-525, 2018.

[62] "EPOXY Resin 1 Gal Kit, General Purpose," [Online]. Available: https://www.amazon.com/dp/B01IU9XYVE/ref=psdc_13399741_t1_B00NLPCA5Y. [Accessed 09 July 2019].

[63] "Water Treatment Ceramsite With Factory Price," [Online]. Available: https://www.alibaba.com/product-detail/Water-Treatment-Ceramsite-With-Factory-Price_60808255387.html?spm=a2700.7724857.normalList.34.430a2a99hQD3Vz. [Accessed 09 July 2019].

[64] "Hydroponic Growing Media Lightweight Expanded Clay Pebbles Pellets," [Online]. Available: https://www.alibaba.com/product-detail/Hydroponic-Growing-Media-Lightweight-Expanded-Clay_60777685703.html?spm=a2700.7724857.normalList.32.1d04daact4Kt9a. [Accessed 09 July 2019].

[65] M. Alazhari, T. Sharma, A. Heath, R. Cooper and K. Paine, "Application of expanded perlite encapsulated bacteria and growth media for self-healing concrete," *Construction and Building Materials,* vol. 160, no. January, pp. 610-619, 2018.

[66] "Lightweight Concrete Expanded Concrete Perlite For Sale," [Online]. Available: https://www.alibaba.com/product-detail/Lightweight-Concrete-Expanded-Concrete-Perlite-For_60775442681.html?spm=a2700.7724857.normalList.1.24b96118i9wdRG. [Accessed 09 July 2019].

[67] "sap hydrogel for agriculture," [Online]. Available: https://www.alibaba.com/product-detail/sap-hydrogel-for-agriculture_60781845485.html?spm=a2700.7724857.normalList.12.3c3658eeosYjC5&s=p. [Accessed 09 July 2019].

[68] "Factory supply white powder Melamine 99.8%," [Online]. Available: https://www.alibaba.com/product-detail/Factory-supply-white-powder-Melamine-99_60806647259.html?spm=a2700.7724838.2017115.11.64bc6efbN9haMr&s=p. [Accessed 09 July 2019].

Appendix A: Sieve Analysis of Aggregates

Golder Associates

SIEVE ANALYSIS OF FINE AND COARSE AGGREGATE

CSA A23.2-2A

LEHIGH MATERIALS, DIVISION OF LEHIGH HANSON MATERIALS LTD.
P.O. Box 1790
Sechelt, BC
V0N 3A0

January 12, 2016
Project Number: 1530704/7000

ATTENTION: Mr. Nick Sawchuk

PROJECT: CSA Concrete Aggregate Testing, December 2015

Sample:	Fine Aggregate
Source:	Sechelt Pit

DATE SAMPLED: December 2015
DATE TESTED: January 6, 2016

SAMPLED BY: Client
TESTED BY: RZ

SIEVE ANALYSIS					MATERIAL SPECIFICATION: CSA FA1	
Sieve Size (mm)	% Retained	% Passing	Individual % Retained (Split values)			
			+ 5	- 5		
10	0.0	100.0	0.0		100	100
5	0.0	100.0	0.0		95	100
2.50	10.3	89.7		10.3	80	100
1.25	17.7	72.0		17.7	50	90
0.630	21.9	50.2		21.9	25	65
0.315	28.6	21.5		28.6	10	35
0.160	16.2	5.3		16.2	2	10
0.080	4.1	1.2		4.1	0	3
PAN	1.2	0		1.2		
Total	100.0		0.0	100.0		

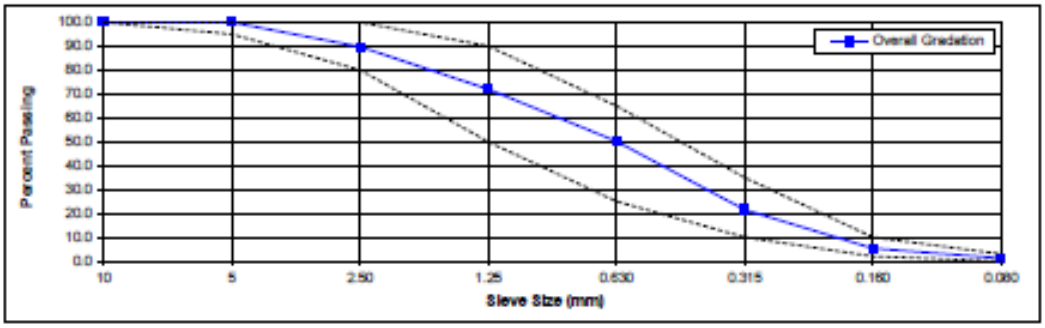

Remarks: Fineness Modulus: 2.61

Reported by: I. Chung

Reviewed by: L. Hu, M.Sc.E., P.Eng.

Notice: The test data given herein pertain to the sample provided, and may not be applicable to material from other production zones/periods. This report constitutes a testing service only. Interpretation of the data given here may be provided upon request.

Appendix B: Coarse Aggregates Relative Density and Absorption

Golder Associates

RELATIVE DENSITY AND ABSORPTION OF COARSE AGGREGATE

CSA A23.2-12A

January 12, 2016
Project Number: 1530704/7000

LEHIGH MATERIALS, DIVISION OF LEHIGH HANSON MATERIALS LTD.
P.O. Box 1790
Sechelt, BC
V0N 3A0

ATTENTION: Mr. Nick Sawchuk

PROJECT: CSA Concrete Aggregate Testing, December 2015

Sample:	**Coarse Aggregate**
Source:	**Sechelt Pit**

Date sampled: December 2015
Date tested: January 12, 2016

Sampled by: Client
Tested by: DC

Trial No.	Mass (g)	Relative Density (Dry Basis)	Relative Density (SSD Basis)	Apparent Relative Density	Absorption (%)
1	3483.4	2.699	2.717	2.748	0.66
2	3808.0	2.690	2.709	2.743	0.72
AVERAGE		**2.695**	**2.713**	**2.746**	**0.69**

Reported by: I. Chung

Reviewed by: _____
L. Hu, M.Sc.E., P.Eng.

GOLDER ASSOCIATES LTD., 300 - 3811 North Fraser Way, Burnaby, BC Canada V5J 5J2 Tel: 604-412-6899 Fax: 604-412-6816

Appendix C: Fine Aggregates Relative Density and Absorption

Golder Associates

RELATIVE DENSITY AND ABSORPTION OF FINE AGGREGATE

CSA A23.2-6A

January 12, 2016
Project Number: 1530704/7000

LEHIGH MATERIALS, DIVISION OF LEHIGH HANSON MATERIALS LTD.
P.O. Box 1790
Sechelt, BC
V0N 3A0

ATTENTION: Mr. Nick Sawchuk

PROJECT: CSA Concrete Aggregate Testing, December 2015

Sample:	**Fine Aggregate**
Source:	**Sechelt Pit**

Date sampled: December 2015
Date tested: January 7, 2016

Sampled by: Client
Tested by: DC

Trial No.	Mass (g)	Relative Density (Dry Basis)	Relative Density (SSD Basis)	Apparent Relative Density	Absorption (%)
1	500.5	2.649	2.669	2.705	0.79
2	500.8	2.652	2.672	2.708	0.78
AVERAGE		**2.651**	**2.671**	**2.707**	**0.79**

Reported by: I. Chung

Reviewed by: _____
L. Hu, M.Sc.E., P.Eng.

Notice: The test data given herein pertain to the sample provided, and may not be applicable to material from other production zones/periods. This report constitutes a testing service only. Interpretation of the data given here may be provided upon request.

GOLDER ASSOCIATES LTD., 300 - 3811 North Fraser Way, Burnaby, BC Canada V5J 5J2 Tel: 604-412-6899 Fax: 604-412-6816

Appendix D: Material Safety Data Sheet for Calcium Lactate

iChemical Technology USA Inc

Material Safety Data Sheet

1. Composition/information on ingredients

Product Name: Calcium lactate

Synonyms:

Company Identification: iChemical Technology USA Inc
1100 Scenic View Trace,Lawrenceville, GA 30044 USA

Telephone Number: 1-336-655-0152

2. Identification of the substance

Catalog Number: EBD8037

CAS #: 814-80-2

Purity: 98%

EINECS#

3. Hazards identification

EMERGENCY OVERVIEW Irritating to eyes, respiratory system and skin.

Potential Health Effects Eye:

Causes eye irritation. May cause chemical conjunctivitis.

Skin:

Causes skin irritation.

Ingestion:

May cause gastrointestinal irritation with nausea, vomiting and diarrhea. The toxicological properties of this substance have not been fully investigated.

Inhalation:

Causes respiratory tract irritation. The toxicological properties of this substance have not been fully investigated. Can produce delayed pulmonary edema.

Chronic:

Effects may be delayed.

4. First aid measures

Eyes:

Immediately flush eyes with plenty of water for at least 15 minutes, occasionally lifting the upper and lower eyelids. Get medical aid.

Skin:

Get medical aid. Flush skin with plenty of water for at least 15 minutes while removing contaminated clothing and shoes. Wash clothing before reuse.

Ingestion:

Never give anything by mouth to an unconscious person. Get medical aid. Do NOT induce vomiting. If conscious and alert, rinse mouth and drink 2-4 cupfuls of milk or water. Wash mouth out with water.

Inhalation:

Remove from exposure and move to fresh air immediately. If not breathing, give artificial respiration. If breathing is difficult, give oxygen. Get medical aid. Do NOT use mouth-to-mouth resuscitation.

Notes to Physician:

Treat symptomatically and supportively.

5. Fire fighting measures

General Information:

As in any fire, wear a self-contained breathing apparatus in pressure-demand, MSHA/NIOSH (approved or equivalent), and full protective gear. During a fire, irritating and highly toxic gases may be generated by thermal decomposition or combustion.

Extinguishing Media:

Use water spray, dry chemical, carbon dioxide, or chemical foam.

6. Accidental release measures

General Information: Use proper personal protective equipment as indicated in Section 8.

Spills/Leaks:

Vacuum or sweep up material and place into a suitable disposal container. Clean up spills immediately, observing precautions in the Protective Equipment section. Avoid generating dusty conditions. Provide ventilation.

7. Handling and storage

Handling:

Minimize dust generation and accumulation. Avoid contact with eyes, skin, and clothing. Keep container tightly closed. Use with adequate ventilation. Wash clothing before reuse. Avoid breathing dust.

Storage:

Store in a cool, dry place. Store in a tightly closed container.

8. Exposure Controls / PPE

Engineering Controls:

Facilities storing or utilizing this material should be equipped with an eyewash facility and a safety shower. Use adequate ventilation to keep airborne concentrations low.

Exposure Limits CAS# **814-80-2**

Personal Protective Equipment Eyes:

Wear appropriate protective eyeglasses or chemical safety goggles as described by OSHA's eye and face protection regulations in 29 CFR 1910.133 or European Standard EN166.

Skin:

Wear appropriate protective gloves to prevent skin exposure.

Clothing:

Wear appropriate protective clothing to prevent skin exposure.

Respirators:

Follow the OSHA respirator regulations found in 29 CFR 1910.134 or European Standard EN 149. Use a NIOSH/MSHA or European Standard EN 149 approved respirator if exposure limits are exceeded or if irritation or other symptoms are experienced.

9. Physical and chemical properties

Physical State:Powder

Color: White

Odor: Not available.

pH: Not available.

Vapor Pressure: Not available.

Viscosity: Not available.

Boiling Point: 227.6 °C at 760 mmHg

Freezing/Melting Point:Not available.

Autoignition Temperature: Not available.

Flash Point: 109.9 °C

Explosion Limits, lower: Not available.

Explosion Limits, upper: Not available.

Decomposition Temperature:Not available.

Specific Gravity/Density: Not available.

Molecular Formula: C6H10CaO6

Molecular Weight: 218.22

10. Stability and reactivity

Chemical Stability:

Stable under normal temperatures and pressures.

Conditions to Avoid:

Dust generation.

Incompatibilities with Other Materials:

Acids, bases, reducing agents, strong oxidizing agents.

Hazardous Decomposition Products:

Carbon monoxide, carbon dioxide,

Hazardous Polymerization: Has not been reported.

11. Toxicological information

RTECS#:

CAS# **814-80-2** unlisted.

LD50/LC50:

Not available.

iChemical Technology USA Inc
TEL: 1-336-655-0152
Email: sales@ichemical.com Website: www.ichemical.com
Address: 1100 Scenic View Trace,Lawrenceville, GA 30044 USA

Carcinogenicity:

Calcium lactate

Not listed by ACGIH, IARC, or NTP.

12. Ecological information

Not available.

13. Disposal consideration

Dispose of in a manner consistent with federal, state, and local regulations.

14. Transportation information

IATA

Shipping Name: Not dangerous goods.

Hazard Class: Not dangerous goods.

UN Number: Not dangerous goods.

Packing Group: Not dangerous goods.

IMO

Shipping Name: Not dangerous goods.

Hazard Class: Not dangerous goods.

UN Number: Not dangerous goods.

Packing Group: Not dangerous goods.

RID/ADR

Shipping Name: Not dangerous goods.

Hazard Class: Not dangerous goods.

UN Number: Not dangerous goods.

Packing group: Not dangerous goods.

15. Regulatory information

European/International Regulations European Labeling in Accordance with EC Directives Hazard Symbols: XI

Risk Phrases:

R 36/37/38 Irritating to eyes, respiratory system and skin.

Safety Phrases:

S 26 In case of contact with eyes, rinse immediately with plenty of water and seek medical advice.

S 37/39 Wear suitable gloves and eye/face protection.

WGK (Water Danger/Protection) CAS#**814-80-2** No information available.

Canada

None of the chemicals in this product are listed on the DSL/NDSL list.

CAS#**814-80-2** is not listed on Canada's Ingredient Disclosure List.

US FEDERAL TSCA CAS# **814-80-2** is not listed on the TSCA inventory.

It is for research and development use only.

iChemical Technology USA Inc
TEL: 1-336-655-0152
Email: sales@ichemical.com Website: www.ichemical.com
Address: 1100 Scenic View Trace,Lawrenceville, GA 30044 USA

16. Other information

The information above is believed to be accurate and represents the best information currently available to us. However, we make no warranty of merchantability or any other warranty, express or implied, with respect to such information, and we assume no liability resulting from its use. Users should make their own investigations to determine the suitability of the information for their particular purposes. In no way shall the company be liable for any claims, losses, or damages of any third party or for lost profits or any special, indirect, incidental, consequential or exemplary

Appendix E: Certificate of Analysis for Calcium Lactate

iChemical Technology USA Inc

Certificate of Analysis

Product Name:	**Calcium lactate**
Catalog Number:	**EBD8037**
CAS Number:	**814-80-2**
Molecular Formula:	**C6H10CaO6**
Molecular Weight:	**218.22**

Test Results

Batch Number:	**2017071405**
Storage condition:	**Room temperature**
Quantity:	**2kg*1**
Appearance:	**White powder**
Boiling point:	**227.6 °C at 760 mmHg**
Melting point:	**N/A**
Flash point:	**109.9 °C**
Assay:	**98%**

Glenn Yang
_____
QC Supervisor

August 08,2017
_____
Acceptance Date

iChemical Technology USA Inc
TEL: 347-443-0500
Email: sales@ichemical.com Website: www.ichemical.com
Address: 1100 Scenic View Trace,Lawrenceville, GA 30044 USA